Check for updates

Advanced Functional Materials

ADVANCED FUNCTIONAL MATERIALS
www.afm-journal.de

REVIEW OPEN ACCESS

Chemically Fueled Systems Chemistry Across Length Scales

Brigitte A. K. Kriebisch | Job Boekhoven

School of Natural Sciences, Department of Bioscience, Technical University of Munich, Garching, Germany

Correspondence: Job Boekhoven (job.boekhoven@tum.de)

Received: 10 February 2026 | **Revised:** 4 July 2026 | **Accepted:** 9 July 2026

Keywords: catalysis | chemical-fueled reaction cycle | chemically fueled materials | chemically-fueled polymers | feedback mechanisms | kinetic asymmetry | self-assembly

ABSTRACT

Inspired by nature, chemically fueled reaction cycles provide a general strategy to couple the dissipation of chemical potential to controlled changes in molecular structure, assembly, and material properties. Here, we review how kinetically stable yet thermodynamically activated fuels, catalytic activation–deactivation cycles, and supramolecular transformations integrate into a common design spanning molecular, assembly, and material length scales. We unify terminology across communities using diverse systems into state-network descriptions that capture reciprocal coupling between chemical and supramolecular states. Central to function is kinetic asymmetry (feedback from the supramolecular state on reaction rates), which biases reaction flux and enables work-like behavior, including directional motion, tunable lifetimes, self-healing, oscillations, bistability, and spatiotemporal control of optical, mechanical, and catalytic properties. By contrasting single-point versus multipoint activation and intramolecular versus intermolecular processes, we extract practical design principles and highlight open challenges, including quantitative kinetic descriptions at the assembly scale, management of waste accumulation under sustained fueling, and scaling chemo-mechanical coupling toward higher-order autonomous systems. Overall, this review provides a shared mechanistic language and a set of transferable guidelines for engineering functional, adaptive, chemically powered systems across all length scales.

1 | Introduction

Over the past decades, synthetic chemists have mastered the design, development, and synthesis of supramolecular systems with dynamic functions, such as the ability to be controlled over space and time, adapt or move, heal themselves, or even perform work. For all of these functions, energy transduction is required. How to make molecules perform work has long been a daunting task, but recent breakthroughs have made it more achievable. One key was taking inspiration from biology, which thrives on its ability to convert energy into work. Life frequently employs chemical reaction cycles to regulate supramolecular processes, thereby performing work efficiently across different length scales. These reaction cycles share the common property of catalyzing the conversion of a molecule with high chemical potential (a fuel) into one with lower chemical potential (a waste molecule). The energy extracted from the fuel-to-waste conversion drives a supramolecular process. For example, the phosphorylation and dephosphorylation of enzymes by ATP as fuel is used to regulate many biological functions like pumping Calcium ions against an ion gradient from the cell inside to the cell outside via the cell membrane by the Ca^{2+} ATPase [1], the kinesin motor [2] that transports intracellular cargo along the microtubule track, the actin-myosin motors that contract and expands the cytoskeleton [3, 4], the dynamic assembly of microtubules and actin filaments [5–7], or the archaeal flagellar motor [8, 9]. Inspired by these biological-fueled processes, researchers coupled non-equilibrium chemical reaction cycles to supramolecular processes, thereby developing synthetic analogs that operate on various length scales, including the molecular scale and the scale of molecular assemblies. Moreover, supramolecular non-equilibrium systems have been developed that are not

This is an open access article under the terms of the Creative Commons Attribution License, which permits use, distribution and reproduction in any medium, provided the original work is properly cited.
© 2026 The Author(s). *Advanced Functional Materials* published by Wiley-VCH GmbH

driven by chemical energy but by light [10–12] or electricity [12–14].

This review focuses on supramolecular systems that convert energy from molecules with high chemical potential to regulate their (material) properties. First, we illustrate the basic design principle of the chemically fueled reaction cycle that underlies the biological and synthetic systems, independent of their length scale. Next, we discuss the motivation for regulating supramolecular systems with fuels from a materials standpoint. We then clarify how the coupling of the chemical reaction cycle to supramolecular processes depends on its scale—the molecular or assembly scale and on the number of reaction sites. Finally, we outline the remaining challenges toward new functional, autonomous, adaptive systems and materials. For similar reviews that focus on energy harvested from light or electrical potential, we refer the reader to other excellent reviews [10, 11, 13, 15].

2 | The Design Principles of the Chemically Fueled Supramolecular Process

In this section, we describe the general design considerations for the chemically fueled supramolecular process at the heart of all the synthetic systems described in this review. We will focus on the design criteria for the chemical fuel, which needs to be kinetically stable yet thermodynamically activated. Next, we examine the design criteria for the catalyst that releases the fuel's chemical potential, the supramolecular process, and the roles of kinetic asymmetry and feedback mechanisms in performing work.

2.1 | The Chemical Fuel: Kinetically Stable and Thermodynamically Unstable

In fueled reaction cycles, a molecule with high chemical potential is converted into a waste molecule with low chemical potential. We introduced the term "fuel" [16] for such a molecule, as it is an intuitive term—it is (practically) irreversibly converted into waste and, ideally, used to perform work, making it similar to the fuels we use in our everyday lives. From this, we can already deduce one requirement—a fuel should be thermodynamically activated, meaning it has the potential to release a large amount of Gibbs free energy. That requirement ensures that we can do work, but also that the conversion is (practically) irreversible. Simultaneously, the fuel should be kinetically stable under the reaction conditions or operating conditions in the absence of the catalyst. That means the fuel should have a large energy barrier to prevent the spontaneous release of free energy. From this perspective, adenosine triphosphate (ATP) is an amazing fuel. It releases 30.5 $kJmol^{-1}$ kJ/mol upon its conversion to adenosine diphosphate (ADP) through hydrolysis [17]. Yet, it requires ~59 KbT (146.5 $kJmol^{-1}$) to do so as determined by DFT calculations [18]. Only by using a catalyst can the energy be released at room temperature. Beyond ATP, the cell uses fuels such as nicotinamide adenine dinucleotide (NADH), guanosine triphosphate (GTP), acetyl-CoA, and others [19].

2.2 | The Catalyst: Liberating the Chemical Potential of the Fuel Through a Catalytic Reaction Cycle

If a fuel is thermodynamically activated but kinetically stable, its energy can only be released on meaningful timescales using a catalyst. Here is where the chemical reaction cycle comes into play. Let us take the Ca^{2+} ATPase as an example of such a catalyst in a reaction cycle [1, 20]. Without the catalyst, ATP has a half-life of several days [21]. However, Ca^{2+}-ATPase has a catalytic center that destabilizes the phosphodiester bond, thereby accelerating ATP hydrolysis. It does so in a series of steps, but we can group them into at least two steps—the catalyst activation and its subsequent deactivation (Figure 1A). In the case of activation, an aspartic acid residue in the catalyst is first phosphorylated, transferring an ATP phosphate group to the ATPase, releasing ADP as a waste. Then, in the deactivation, the phosphorylated ATPase is dephosphorylated by reaction with water, which releases the phosphate group (P_i) as waste. Taken together, the reaction cycle hydrolyzes ATP to ADP and inorganic phosphate, briefly phosphorylating the ATPase. It is important that activation and deactivation occur in a cyclic manner. The ATPase can be reused after a cycle—it is truly a catalyst, accelerating ATP hydrolysis by making it a two-step process and not being consumed itself.

Based on these requirements, several synthetic fuel-driven reaction cycles [11, 22, 23] have been reported in which activation and deactivation are based on oxidation and reduction [24–30], olefin metathesis [31, 32], phosphorylation and dephosphorylation [33–45], methyl ester formation and hydrolysis [16, 46, 47], anhydride formation and hydrolysis [25, 48–58], activated ester formation and hydrolysis [47, 59, 60], transacylation [44, 61, 62], imine formation and hydrolysis [63], and others [64–66].

2.3 | The Supramolecular Process

Following the design principles above, we can deduce that the chemical fuel liberates its chemical potential, thereby driving a chemical reaction cycle. From the catalyst's perspective, a state with a higher chemical potential is temporarily reached. If, in the activated state, the catalyst changes its function, the chemical potential released during the fuel-to-waste reaction temporarily alters its function. One may wonder, what is the point if the deactivation reverts the catalyst to the original state? Why not create a permanently active function? Coupling a function to a chemical reaction cycle allows for control. For example, the cell in which the catalyst resides can control which enzyme is active at what time in a cell cycle and for how long. Moreover, by applying a gradient of fuel, a cell can control where an enzyme is activated, offering critically important spatiotemporal control. Thus, at the simplest level, coupling a change of function to a chemically fueled reaction cycle enables their spatio-temporal regulation (Figure 1B).

However, we can do much more with a chemical reaction cycle if we couple the cycle with a supramolecular process (Figure 1C). For example, when one attaches the catalytic motifs for the fuel conversion to a supramolecular motif, one can regulate the supramolecular state of a system using the chemical reaction

16163028, 2026, 68, Downloaded from https://advanced.onlinelibrary.wiley.com/doi/10.1002/adfm.77237, Wiley Online Library on [17/11/2026]. See the Terms and Conditions (https://onlinelibrary.wiley.com/terms-and-conditions) on Wiley Online Library for rules of use; OA articles are governed by the applicable Creative Commons License

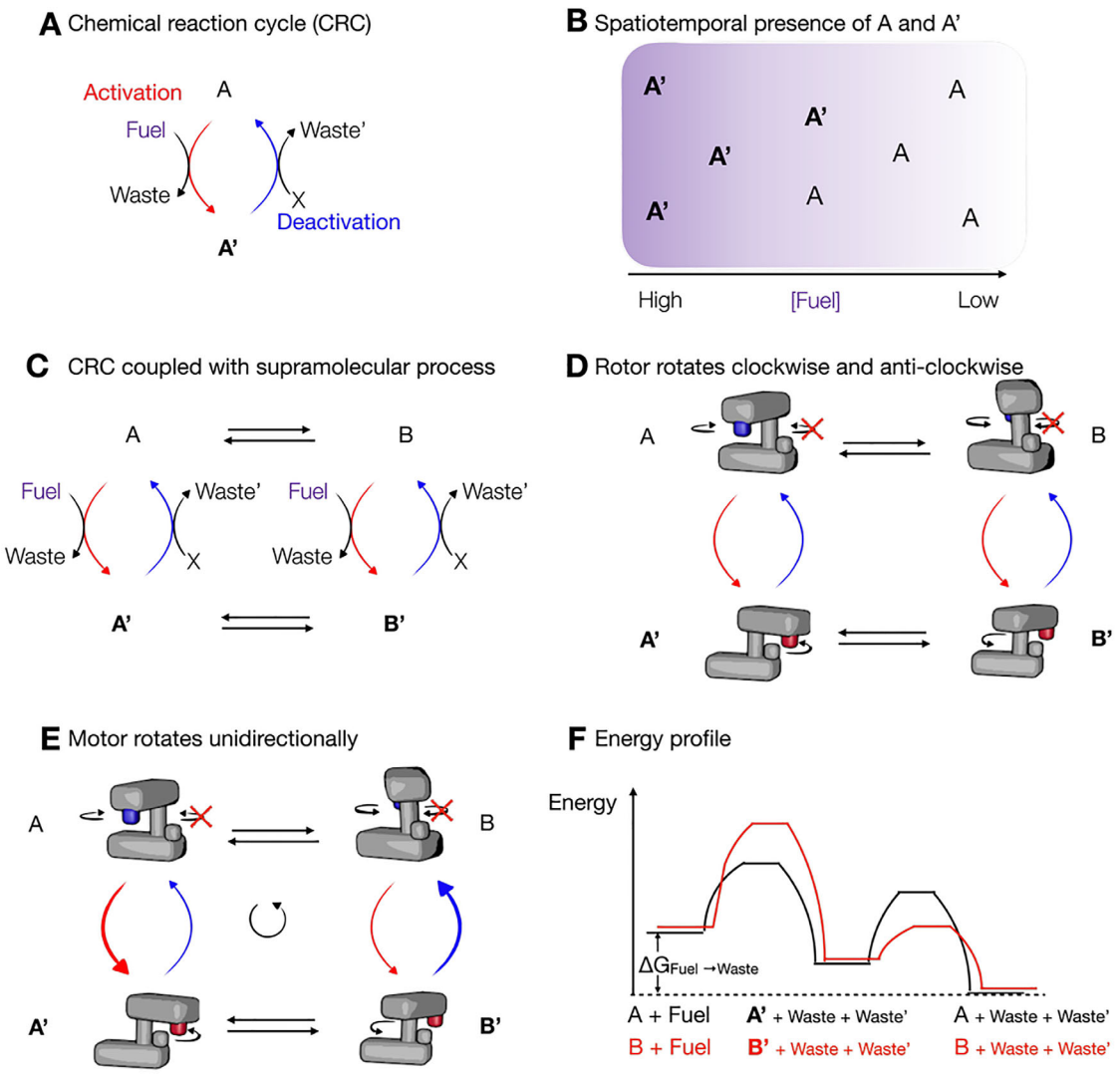

FIGURE 1 | The design principles of chemically fueled supramolecular processes. (A) A simple chemical-fueled reaction cycle. (B) The fuel concentration regulates the spatiotemporal presence of A and A'. (C) Coupling the chemically fueled reaction cycle with a supramolecular process. The four-step reaction scheme illustrates how the chemical reaction cycle can regulate the supramolecular state. (D) A molecular rotor rotates clockwise and anti-clockwise at equal rates if no kinetic asymmetry is present. (E) The example of the molecular motor shows that to perform, i.e., to rotate unidirectionally, we need the presence of kinetic asymmetry—activation needs to be faster in state A and/or deactivation faster in state B. (F) The energy profile of state A reacts with fuel vs state B reacts with fuel.

cycle [67–69]. In these systems, we can distinguish four states. In state A, the catalyst is neither activated nor engaged in a supramolecular process (state A, Figure 1C). Upon reaction with fuel, it activates to the higher energy state—it is activated but not engaged in a supramolecular process (state A'). From there, the activated catalyst can undergo a supramolecular transformation to reach state B', i.e., it undergoes a chemical process in which no new covalent bonds are formed, but, instead, non-covalent interactions play a role (state B'). For example, it can change its conformation [70–72], it assembles [73–75], folds [76–78], or contracts [79–82]. Finally, the activated state engaged in the supramolecular process can deactivate, yielding state B, in which the deactivated state is engaged in the supramolecular process. When designed correctly, the catalyst's thermodynamically unfavored supramolecular state (state B) can be accessed by first activating it (state A'). That way, the supramolecular function can be where and when fuel is present.

Above, we describe the network of four states moving clockwise from A to B. However, that is a highly idealized and practically implausible scenario—each step in the network can also move in the counterclockwise direction. For example, the activated state A' can deactivate to state A without engaging in the supramolecular process. To make matters even more complicated, each activation and deactivation step is technically reversible—the activation state can deactivate by liberating a fuel molecule. However, in practice, as we discussed above, reversibility is typically not considered because it is highly unfavored.

2.4 | Feedback of the Supramolecular State on the Reaction Cycle Yield Kinetic Asymmetry

As we described above, each chemically fueled supramolecular process has four states, and the cycle can operate in either

16163028, 2026, 68, Downloaded from https://advanced.onlinelibrary.wiley.com/doi/10.1002/adfm.77237, Wiley Online Library on [17/11/2026]. See the Terms and Conditions (https://onlinelibrary.wiley.com/terms-and-conditions) on Wiley Online Library for rules of use; OA articles are governed by the applicable Creative Commons License

clockwise or counterclockwise direction. In a scenario in which activation occurs at exactly the same rates in the supramolecular engaged or disengaged state, and also deactivation occurs at exactly the same rates in the supramolecular engaged or disengaged state, these cycles operate at equal rates clockwise and counterclockwise. However, the overall reaction rates should be asymmetric—the clockwise rate should be faster or slower than the counterclockwise rate [83, 84]. We explain the importance of rate asymmetry using an intuitive example—a molecular motor (Figure 1D,E) [85, 86]. A molecular motor has a rotor and a stator, with the rotor rotating relative to the stator. In the non-activated state (state A) the rotor can point toward us, or it can rotate clockwise 180° to point away from us (state B). A is hindered from rotating counterclockwise to B by a bulky group. When chemically activated, A becomes A'. Now, the rotor can rotate 180° counterclockwise to A' to B', but not clockwise. For simplicity, let's make the equilibrium position between A and B, and A' and B' equal, such that each state is occupied equally. Upon application of chemical fuel, the cycle and, thus, the motor rotates clockwise and counterclockwise at exactly the same rate, and no work is performed—a rotor (Figure 1D). If, however, activation is fast in state A and slow in state B, due to a difference in the Gibbs free activation energy barrier, the rotor is more likely to rotate clockwise than counterclockwise. Or, if deactivation is faster in state B than in state A, it rotates oppositely (Figure 1E,F).

From the explanation above, we understand that the mechanical state should affect the catalyst's activation and deactivation rates to obtain kinetic asymmetry. This holds for molecular motors and other molecular machines, but it is also true for molecular assembly, where multiple molecules interact through non-covalent interactions. As the field of molecular machines and chemical-fueled self-assembly developed independently, they referred to the process differently. In the field of molecular machines, the terms "kinetic asymmetry" [87–89], "ratcheting" [90–92], and "kinetic gating" [87–92] are especially used, and we refer to some excellent recent reviews here [93, 89]. In the field of molecular self-assembly, the process of accelerating and decelerating chemical reactions by the supramolecular state was described from the point of view of the assembly. The assembled state exerts feedback on the reaction kinetics of the reaction cycle, thus altering its fate. Thus, the term feedback is more commonly applied, i.e., the supramolecular state exerts feedback on its activation and/or deactivation. Specifically, four different modes of feedback can be distinguished [73, 74]: the supramolecular state can exert:

1) Negative feedback (decelerates) on its activation. We refer to this as a self-inhibition mechanism [73].
2) Positive feedback (accelerates) on its activation. We refer to this as a self-amplification or autocatalytic mechanism [31, 73, 94, 95, 74].
3) Negative feedback (decelerates) on its deactivation. We refer to this as a self-protection mechanism [73, 74, 96–98].
4) Positive feedback (accelerates) on its deactivation. We refer to this as a self-destruction mechanism [73, 74].

Besides the term "feedback", the field of molecular self-assembly has also used the terms "reciprocal coupling" [59], "cooperative catalysis" [59], or "catalysis" [73]. Independent of the nomenclature (kinetic asymmetry or feedback mechanisms), the principles remain the same—the supramolecular engaged state should have different activation and deactivation rates to perform work using the chemical fuel.

3 | Motivation for Chemically Fueled Supramolecular Processes

Nature's ability to control and regulate proteins to perform diverse tasks like pumping (Ca^{2+} ATPase) [1], generating pushing and pulling forces (microtubules) [5–7], or transporting cargo (kinesin-motor) [2] through coupling chemical reaction cycles with the mechanical state of proteins, has motivated scientists to exploit this concept for synthetic systems. By spatiotemporally controlling the mechanical state and structure of small molecules, macromolecules, or nanoparticles reversibly, scientists aim to develop advanced materials, such as molecular synthesizers, sensors, or cargo-transporting nanorobots that respond to environmental cues. The literature reviewed in the following sections shows how far the field has come, the influence of the length scale, and the challenges ahead.

4 | Coupling the Chemically Fueled Reaction cycle Supramolecular Process on Different Length Scales

From the section above, it became clear how chemically fueled reaction cycles can populate an equilibrium with spatiotemporal control or perform work by asymetry in the reaction rates in the chemical reaction cycle. In the following sections, we describe how chemically fueled reaction cycles can regulate supramolecular processes. We subdivide this section based on the length scale of the supramolecular process, whether inter- or intramolecular. For example, the chemically-fueled reaction cycle can regulate the folding of the catalyst (Figure 2A). That way, the catalyst can be in four states, i.e., activated or deactivated, and folded or unfolded. A 2 × 2 matrix yields a four-state model. We will clarify such scenarios using experimentally reported systems, like the folding of a DNA hairpin or the rotation around a bond by a molecular motor. We can increase the complexity of the scenario if the catalyst can assemble with other catalysts (Figure 2B). When we describe this from the perspective of one catalyst molecule, it can still only be activated or deactivated, but it can now be assembled with 1, 2, 3, or n building blocks. We can represent this scene as a 2 × n matrix. Again, we demonstrate this through experimental systems such as the self-assembly of chemically activated molecules into fibers or vesicles. Then, we further subdivide based on whether the catalyst can be activated multiple times, like in the case of polymers or nanoparticles, which we refer to as multipoint activation. These multipoint catalysts can fold or dimerize, in which case there are only two supramolecular states, i.e., n × 2 states (Figure 2C). We will describe experimental systems in which a polymer strand can fold, but only when a large part of its monomers is activated. Finally, such multipoint activation catalysts can assemble into architectures with thousands of building blocks, in which case we refer to m × n states. Here, we make our point with experimental systems in which nanoparticles can assemble into nanoparticle

16163028, 2026, 68, Downloaded from https://advanced.onlinelibrary.wiley.com/doi/10.1002/adfm.77237, Wiley Online Library on [17/11/2026]. See the Terms and Conditions (https://onlinelibrary.wiley.com/terms-and-conditions) on Wiley Online Library for rules of use; OA articles are governed by the applicable Creative Commons License

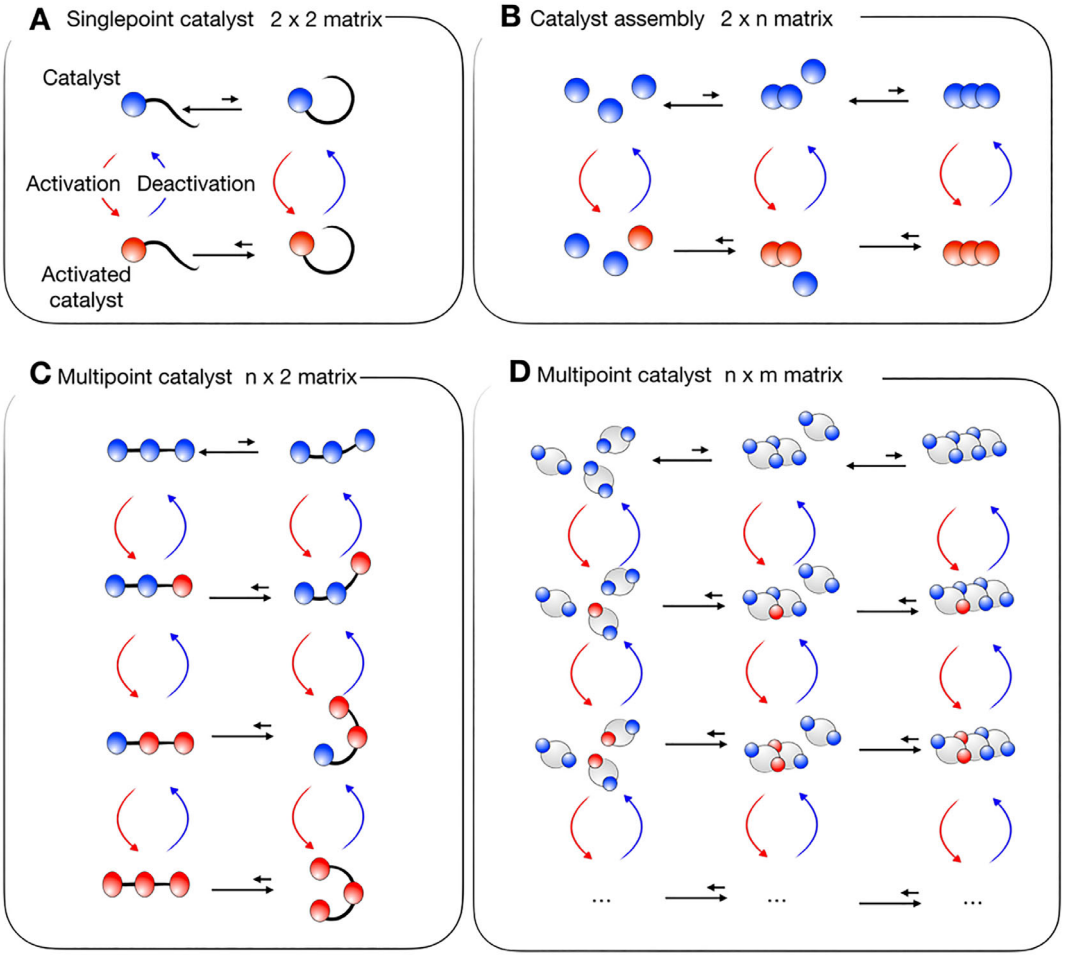

FIGURE 2 | Coupling the chemical reaction cycle to different length scales. (A) The chemical reaction cycle regulates intramolecular processes via a single catalytic site. This process can be described with a four-state, i.e., 2 × 2 state model. (B) The chemical reaction cycle regulates intermolecular processes via a single catalytic site. This process results in molecular self-assembly, which can be described with a 2xn state model. (C) The chemical reaction cycle regulates intramolecular processes through multiple catalytic sites. This process can be described with a nx2 state model. (D) The chemical reaction cycle regulates intra- and intermolecular processes through multiple catalytic sites. This process can be described with a nxm state model.

clusters but only if a large fraction of their functional groups on their surface is activated.

We focus on this subcategorization as the underlying principles and theory, as well as the expected behavior, strongly depend on the subcategory the system falls into. For example, a molecular motor can be described best by systems of intramolecular single-point activation (Figure 2A). For these four-state models, the kinetic and supramolecular behavior is well-described. In contrast, if a supramolecular polymer shows dynamic instabilities or treadmilling is targeted, it can be best described by intermolecular single-point activation (Figure 2B). Finally, when larger building blocks are required to form a material, such as nanoparticles or polymers, multiple catalyst activation is required (Figure 2C,D).

4.1 | Regulating Intramolecular Processes Through One Catalytic Site

In this section, we focus on examples in which chemical-fueled reaction cycles regulate an intramolecular supramolecular process involving small molecules that bear a single catalytic site. For example, the chemical activation could populate a supramolecular equilibrium that involves the folding of the small molecule [76–78] or a molecule's conformational change [70–72]. These examples can be well characterized using the four-state or 2 × 2-state model (Figure 2 A). We subcategorize the examples based on the function these intramolecular steps aim to achieve, i.e., controlling a molecule's optical properties through folding, directional rotation around a bond, or synthesizing a thermodynamically unfavored molecule.

4.1.1 | Chemically Fueled Folding to Regulate Material Properties

In biology, proteins fold into three-dimensional shapes. Through this folding, proteins adopt dynamic conformational ensembles that give rise to diverse functions, including catalysis, molecular recognition, and signal transduction [99]. These functional states are frequently regulated through ATP-driven phosphorylation and dephosphorylation, which modulate protein conformations and intermolecular interactions. In some cases, phosphorylation can also induce the folding of intrinsically disordered proteins.

16163028, 2026, 68, Downloaded from https://advanced.onlinelibrary.wiley.com/doi/10.1002/adfm.77237, Wiley Online Library on [17/11/2026]. See the Terms and Conditions (https://onlinelibrary.wiley.com/terms-and-conditions) on Wiley Online Library for rules of use; OA articles are governed by the applicable Creative Commons License

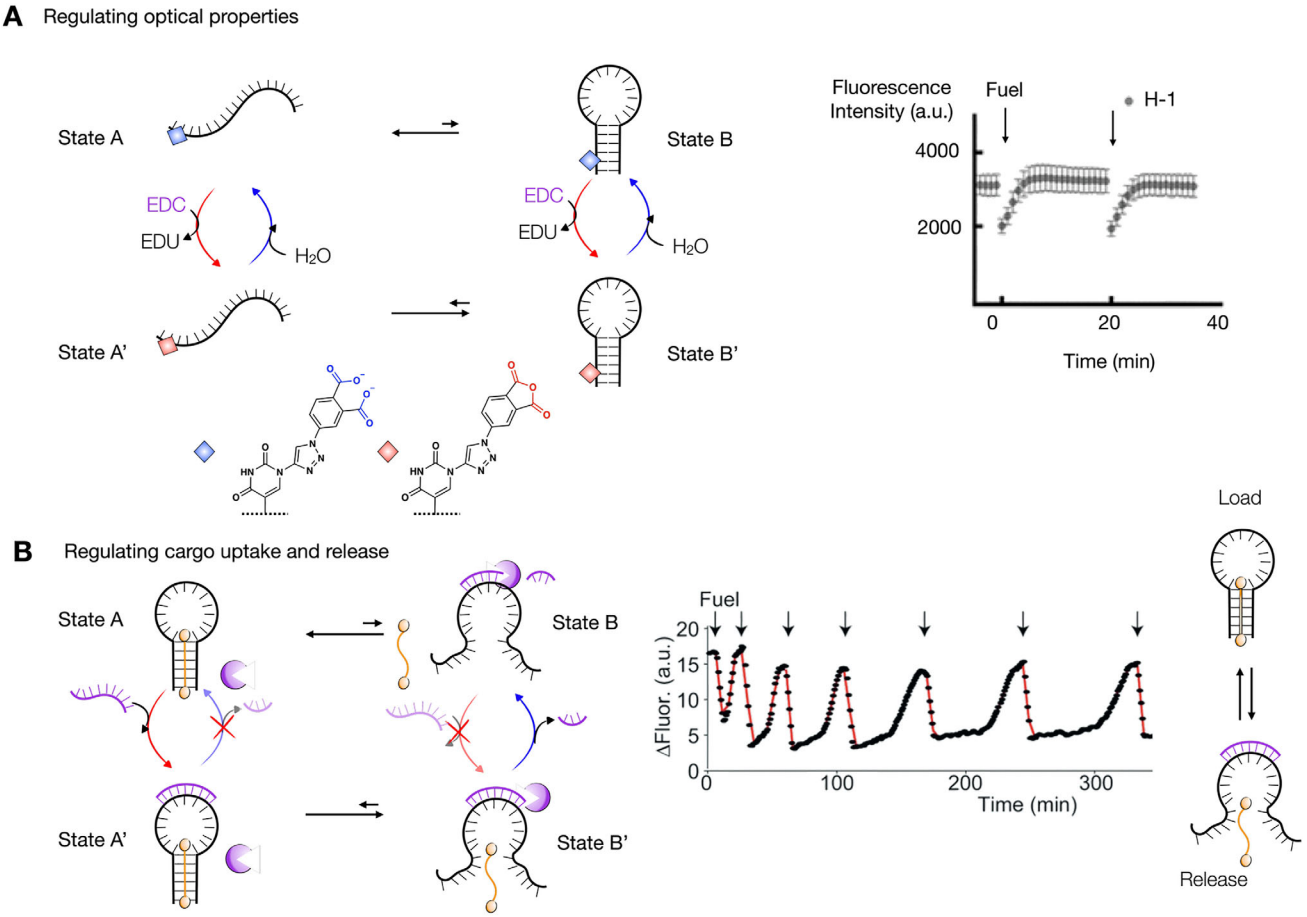

FIGURE 3 | Chemically fueled folding. (A) Chemically-fueled conformational control of DNA hairpin opening and closing. The molecular state displays negative feedback on the chemically fueled reaction cycle. Adapted with permission from the authors. (B) An RNA-driven (violet strand) reaction cycle to the conformational flipping of a synthetic DNA-based receptor (grey/blue strand) that can bind or release a molecular cargo (orange strand) depending on its conformational state. The kinetic trace shows the reversible transient release of the cargo from the DNA-based receptor after the sequential addition of the fuel strand in the presence of enzyme RNase H. Adapted with permission [77].

For example, multisite phosphorylation drives the folding of an intrinsically disordered protein involved in translation [100, 101]. Inspired by such control, researchers used this approach to control the conformational states of molecules and, thereby, the molecular properties [76–78]. Below, we highlight examples of such control over molecular properties using a carbodiimide-fueled reaction cycle.

For example, a carbodiimide-driven reaction cycle can be coupled to the folding of a DNA hairpin to control its fluorescence quenching (Figure 3A) [76]. In this 2 × 2 state system, a catalytic dicarboxylate-modified thymine base is incorporated into a 30-base oligomer DNA strand that bears on 5' end a fluorophore (Cy3 dye) and on the 3' end a quencher (Black Hole Quencher 2). In the deactivated catalyst state, the open, unstructured DNA strand form is thermodynamically favored (state A) due to electrostatic repulsion and steric hindrance. When the carbodiimide fuel is added, the catalyst activates, and the activated state A' forms. In this non-charged activated catalyst state A', the reduced electrostatic repulsion lowers the energy barrier for folding the DNA strand (state B') into a hairpin. In this folded state, the quencher is in close proximity to the fluorophore, quenching its fluorescence. Upon catalyst deactivation, the DNA hairpin (state B) destabilizes and unfolds (state A). The fluorophore is not quenched anymore. Another cycle of folding/unfolding can be restarted. Importantly, the authors found that the closed, folded DNA state protects the activated catalyst from deactivation, thereby exerting negative feedback on the reaction cycle. In other words, the catalyst's supramolecular state affects its reaction rates. Spatola et al. [102] and Zong et al. [103] used a similar approach to regulate the fluorescence properties of small molecules. Here, a trichloroacetic acid-driven and a carbodiimide-driven reaction cycle "locked" and "unlocked" the conformational state of the molecule, which changes the fluorescence emission.

Besides controlling a molecule's optical properties, the chemical-fueled folding can also be powerful for the development of therapeutics that can capture and or release a cargo. For instance, Grosso et al. [77] coupled an RNA-driven reaction cycle to the conformational flipping of a synthetic DNA-based receptor that can bind or release a molecular cargo depending on its conformational state (Figure 3B). In this system, the catalyst is a clamp-like DNA-based receptor (state A). In this state A, the catalyst can bind 9-base DNA cargo through Hoogsteen and Watson-Crick-Franklin interactions and form a triplex structure. Upon activation by an 18-base RNA strand that binds to the

16163028, 2026, 68, Downloaded from https://advanced.onlinelibrary.wiley.com/doi/10.1002/adfm.77237, Wiley Online Library on [17/11/2026]. See the Terms and Conditions (https://onlinelibrary.wiley.com/terms-and-conditions) on Wiley Online Library for rules of use; OA articles are governed by the applicable Creative Commons License

loop portion of the catalyst (state A'), the catalyst undergoes a conformational change: it opens (state B') and releases the DNA cargo. The endoribonuclease enzyme RNase H that binds selectively to the RNA/DNA heteroduplex formed between the DNA loop (catalyst) and the RNA strand (fuel) hydrolyses the RNA strand (fuel) (state B) selectively. Importantly, the enzyme only hydrolyses the RNA strand when bound to the catalyst. In other words, the catalyst's state strongly affects reaction rates. From this kinetic asymmetry, ratcheting occurs, which drives a forward-stepping in the cycle: state A → state A' → state B' → state B → state A. In this system, the catalyst is a receptor that transduces the free energy liberated from the RNA strand fuel to continually bind and release a DNA cargo.

4.1.2 | Chemically Fueled Unidirectional Motion

More recently, scientists have coupled non-equilibrium reaction cycles with single molecules to develop molecular machines that exhibit unidirectional motion at the molecular level, similar to the behavior observed in biological systems [104]. Biological machines like the Ca^{2+}-ATPase pump show kinetic gating, i.e., the supramolecular process reciprocally couples to the reaction cycle as activation and deactivation rates depend on the machine's mechanical status. Under a constant energy supply, the overall kinetic bias the forward-stepping of the machine [70, 71, 86, 105]. Most synthetic analogues of molecular machines operate by sequentially adding various reagents such that the machine activates by adding stimuli and deactivates to the original state when the opposite stimulus is added. For example, by using ion binding [106, 107], redox chemistry [108] or acid-base chemistry [109–111]. In contrast to biological machines, these synthetic machines do not operate autonomously under a constant energy supply. To achieve this autonomous motion, Leigh and coworkers coupled a carbodiimide-fuel-driven reaction cycle [70, 71] and Fmoc-Cl-driven [72] cycle with a molecular system that undergoes a continuous series of conformational changes. As in biological machines, the conformational state exerts feedback on the activation and deactivation rates, thus biasing the machine's forward-stepping. Doing this enables the building of a molecular motor that continuously, directionally rotates 360° upon energy consumption [70], the building of a molecular pump that pumps macrocycles from the bulk solution on a molecular axle [72], and the building of a molecular track on which a macrocycle is displaced directionally [71].

For example, Borsley et al. [70] coupled a carbodiimide-driven reaction cycle to the autonomous, continuous, directional 360° rotation of two aromatic rings around the covalent single bond that connects them (Figure 4). The catalyst, a simple 26-atom biaryl compound (1-phenylpyrrole 2,2′-dicarboxylic acid), catalyzes the carbodiimide conversion into the urea waste. In the activated catalyst state B', the two aromatic rings are covalently connected via an intramolecular anhydride. Activation and deactivation of the catalyst occur incessantly in the presence of carbodiimide fuel. The authors showed that four different conformational catalyst states are present and that the catalyst state strongly affects the reaction rates of activation and deactivation, i.e., activation and deactivation occur faster through particular rotamers of the biaryl system (Figure 4). The activation is faster in state A, and the deactivation is faster in state B' (Figure 4), when (*R,R*)-2 fuel is present. This asymmetric catalysis results in ratcheting—without is clockwise and counterclockwise rotation would be equally fast resulting in a rotor rather than a motor. The chirality of the carbodiimide fuel determines the ratcheting direction and, with this, the directionality of rotation around the covalent bond. In other words, when fueled with (*S,S*)-2, the ratcheting occurs in the opposite direction. In this synthetic system, the catalyst is a motor that transduces the free energy liberated in the carbodiimide-to-urea conversion to drive the net 360° directional rotation of the rotor around the stator. In future work, the simple motor design may enable coupling this molecular motor with larger-scale components [112], thereby performing work across length scales. Thereby, chemical fuel on the nanometer scale can be exploited to power micron-sized machinery.

Borsely et al. [71] and Amano et al. [72] used a similar approach of kinetic gating, i.e., ratcheting, to achieve directional displacement of a macrocycle on a molecular track and to pump macrocycles on a molecular axle. Such systems are typically referred to as molecular information ratchets or catalysis-driven ratchets, because the information that populates intermediates of the chemical reaction network dictates the network's directionality. These systems typically operate under a constant energy supply, i.e., under steady-state conditions. We refer the reader to the review by Amano et al. [84] for an excellent discussion on the underlying ratchet mechanism.

4.1.3 | Utilizing Chemical Fuel to Regulate an Endergonic Synthesis

Large biomolecules, like proteins or DNA, are rich in functional groups and are synthesized from simpler building blocks. These molecules are often thermodynamically unfavored and therefore must be synthesized through endergonic reactions [113]. To facilitate these reactions, they can be coupled to an exergonic (energy-releasing) reaction [89, 19, 114]. Moreover, given the rich nature of the functional groups, the synthesis must be guided along a specific synthetic route. For example, proteins are synthesized by condensing amino acids, even though the reverse reaction is thermodynamically more favored. The ribosome synthesizes proteins through a process that consumes GTP, and the associated GTP hydrolysis provides part of the overall energy input required for directional and accurate protein synthesis [115, 116]. Moreover, it also ensures that the right amino acid is added at the right time as encoded in the RNA it is translating. In other words, the free energy released in the GTP hydrolysis pays the entropic cost of the correct protein synthesis.

Using an exergonic reaction to guide an endergonic chemical reaction has been applied to synthesize thermodynamically unfavorable Diels-Alder products [117, 118]. In two studies, Olivieri et al. [117] and Al Shehimy et al. [118] coupled the Diels-Alder reaction between a diene and dienophile to the exergonic carboxylate-catalyzed carbodimide-to-urea conversion. In the first example [117], the authors tested the Diels-Alder reaction of furanacetic acid with acrylic acid in the absence of a directing group, yielding low conversion because the equilibrium position

16163028, 2026, 68, Downloaded from https://advanced.onlinelibrary.wiley.com/doi/10.1002/adfm.77237, Wiley Online Library on [17/11/2026]. See the Terms and Conditions (https://onlinelibrary.wiley.com/terms-and-conditions) on Wiley Online Library for rules of use; OA articles are governed by the applicable Creative Commons License

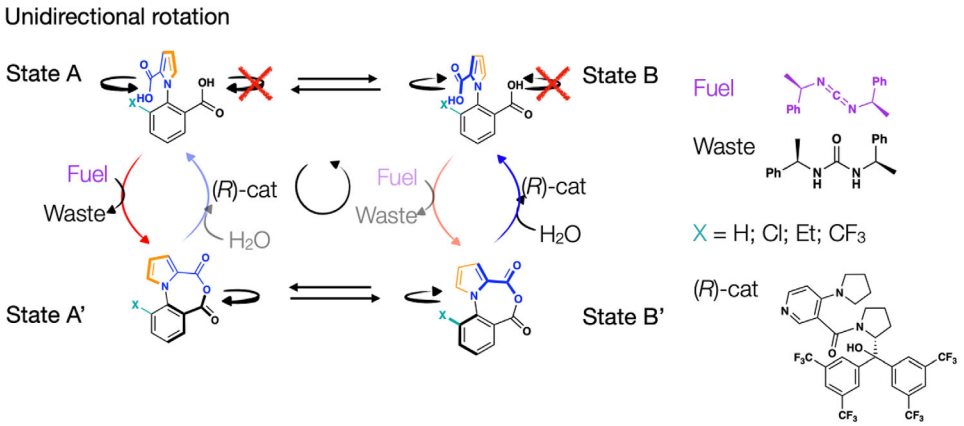

FIGURE 4 | Chemically fueled unidirectional rotation. Autonomous, continuously fueled directional rotation of the rotor (pyrrole-2-carbonyl) around the stator (phenyl-2-carbonyl) for 1-arylpyrrole 2,2′-dicarboxylic acids. Adapted with permission [70].

favors the reactants. Moreover, four possible Diels-Alder products were formed (Figure 5A). However, when the authors used the carbodiimide-driven reaction cycle, the carboxylic acids on the dienophile and the diene (state A) catalyze the carbodiimide-to-urea conversion and thereby get activated to the anhydride state (state A'). The transient anhydride bond temporarily brings the dienophile and diene in proximity (state A'). This tethered intermediate form (state A') increases the effective concentration of the Diels-Alder substrates, making the Diels-Alder reaction an intramolecular downhill process, thereby accelerating the Diels-Alder reaction. Subsequently, the labile anhydride-based Diels-Alder product (state B') hydrolyzes to the energetically uphill Diels-Alder product (state B). In another example [118], the carbodiimide-to-urea conversion is coupled to the unfavored Diels-Alder reaction of furan-based dienes and the dienophile maleic acid (state A, Figure 5B). In both examples, the free energy released from carbodiimide hydration pays the costs of the Diels-Alder reaction. This strategy enables the synthesis of molecules that are energetically uphill with high selectivity, powered by chemical fuels [114].

4.2 | Regulating the Self-Assembly of Molecules Through a Catalytic Site

We described examples in which chemical reaction cycles are coupled to a supramolecular process. In this section, we move up a step in the length scale and examine the implications when the chemical reaction cycle regulates intermolecular interactions that lead to molecular self-assembly. In so-called chemically fueled self-assembly [119, 120], catalysts for the chemical reaction cycle are designed to interact via noncovalent interactions, driving their assembly. Ideally, the catalyst in its non-activated state does not assemble, i.e., the equilibrium position for the state A to state B lies to the left. Upon its activation, the activated catalyst A' is much more likely to assemble, i.e., the equilibrium position lies to the right. There is no assembly when no chemical fuel is present. When fuel is present, the A' and B' equilibrium is populated, leading to the assembly of molecules (Figure 6A).

The four-state model, as we discussed for the intramolecular processes, suggests that there are only two equilibrium constants for the supramolecular process. The situation for chemically fueled self-assembly is much more complicated and can be described loosely by a 2xn-state model (Figure 2B). Where such a model breaks apart is when self-assembly is a cooperative process in which a nucleation barrier must be overcome before self-assembly can occur. Similarly, assembled molecules can become kinetically trapped, which hinders their disassembly [121]. Moreover, the chemical state of a molecule's neighbor also influences the equilibrium constant for assembly, i.e., residing in an assembly of activated or deactivated molecules. In other words, the 2xn-state model can help determine the directionality of chemically fueled processes, but is still in its infancy.

In the last decades, chemically fueled assembly has been used for regulating structure formation, transitions, and degradation of diverse assembly types, fibers [46, 59, 96, 122–124], colloids [79, 96, 98, 125], coacervate [43, 124, 126–128], DNA- [129], and oil-based droplets [95, 97, 124, 130, 131], vesicles [40, 42, 132, 133], micelles [134], and crystals [124, 135]. The following section presents selected examples of chemically fueled molecular self-assembly and explains why the presence of feedback mechanisms within the assemblies is crucial for performing work or storing energy.

4.2.1 | Chemically Fueled Assemblies Can be Dynamic

When the activated catalyst can assemble, but the non-activated catalyst cannot, the resulting assemblies are endowed with properties we usually do not observe in equilibrium. For example, the assemblies can be dynamically restructured [136]. In biology, ATP-binding activates the globular (G)-actin to assemble into actin filaments. The bound ATP hydrolyses to ADP and P_i in the assembled filamentous (F)-actin state. The P_i subsequently dissociates from the F-actin subunit. The affinity of the ADP-bound F-actin is lower and, thus, is prone to disassembly. The original G-actin monomer that binds ATP gets recycled [137, 138].

An early example reported the fuel-driven formation of dynamic fibers [46]. A MeI-driven reaction cycle was coupled to the assembly and disassembly of the small molecule dibenzoyl-L-cysteine (DBC) into fibers (Figure 6A) [46, 16] This system can

16163028, 2026, 68, Downloaded from https://advanced.onlinelibrary.wiley.com/doi/10.1002/adfm.77237, Wiley Online Library on [17/11/2026]. See the Terms and Conditions (https://onlinelibrary.wiley.com/terms-and-conditions) on Wiley Online Library for rules of use; OA articles are governed by the applicable Creative Commons License

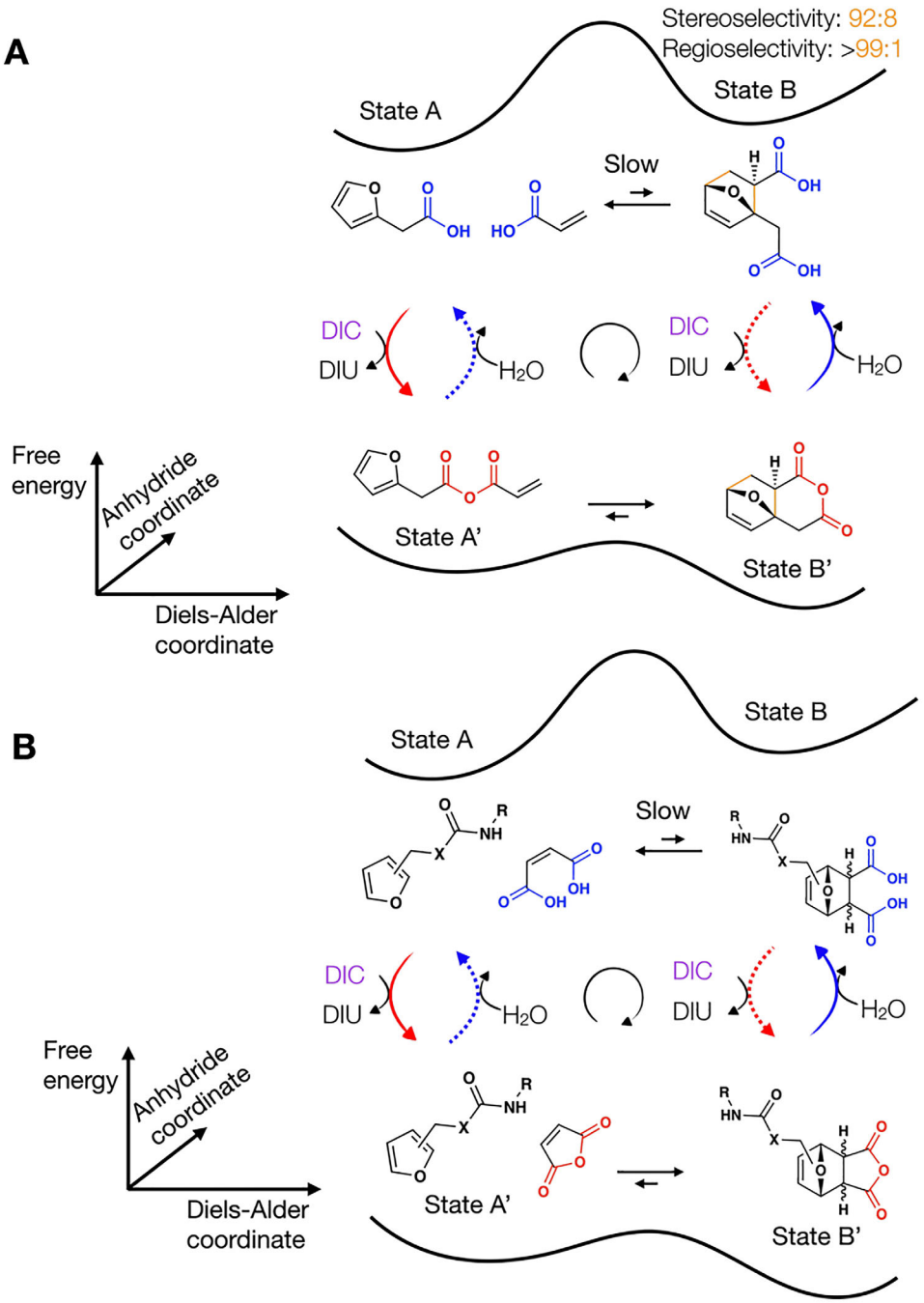

FIGURE 5 | Chemically fueled endergonic synthesis. (A, B) Chemical fuel-driven endergonic synthesis of Diels-Alder products (A) by Olivieri et al. [117] and (B) S. Al Shehimy et al. [118]. Adapted with permission.

best be described by a 3xn-state model. However, when we describe a single catalyst molecule, we can reduce it to the 3 × 2-state model. In this system, the DBC catalyst (state A) catalyzes the MeI-to-MeOH formation under basic aqueous conditions. The MeI fuel methylates the carboxylates of the DBC catalyst, and the corresponding DBC-diester catalyst forms (activation, state A″). The DBC-diester catalyst hydrolyzes to its original catalyst state A, releasing two MeOH molecules. The electrostatic repulsion between the DBC molecules is too high for their assembly. Activation into the DBC-diester catalyst state A″ negates the two negative charges and thus lowers the energy barrier for the activated DBC-diester to self-assemble into nanofibers (state B″). Deactivation of the DBC-diesters in the fiber gives rise to a thermodynamically unstable fiber that can rapidly disassemble from the fiber tips or remain kinetically trapped (state B) (Figure 6B). Moreover, in the presence of MeI fuel, the fiber can grow if a newly activated DBC catalyst assembles at the fiber tips. Thus, the energy released from the MeI-to-MeOH conversion is partially used to form dynamic fibers that grow and collapse.

16163028, 2026, 68, Downloaded from https://advanced.onlinelibrary.wiley.com/doi/10.1002/adfm.77237, Wiley Online Library on [17/11/2026]. See the Terms and Conditions (https://onlinelibrary.wiley.com/terms-and-conditions) on Wiley Online Library for rules of use; OA articles are governed by the applicable Creative Commons License

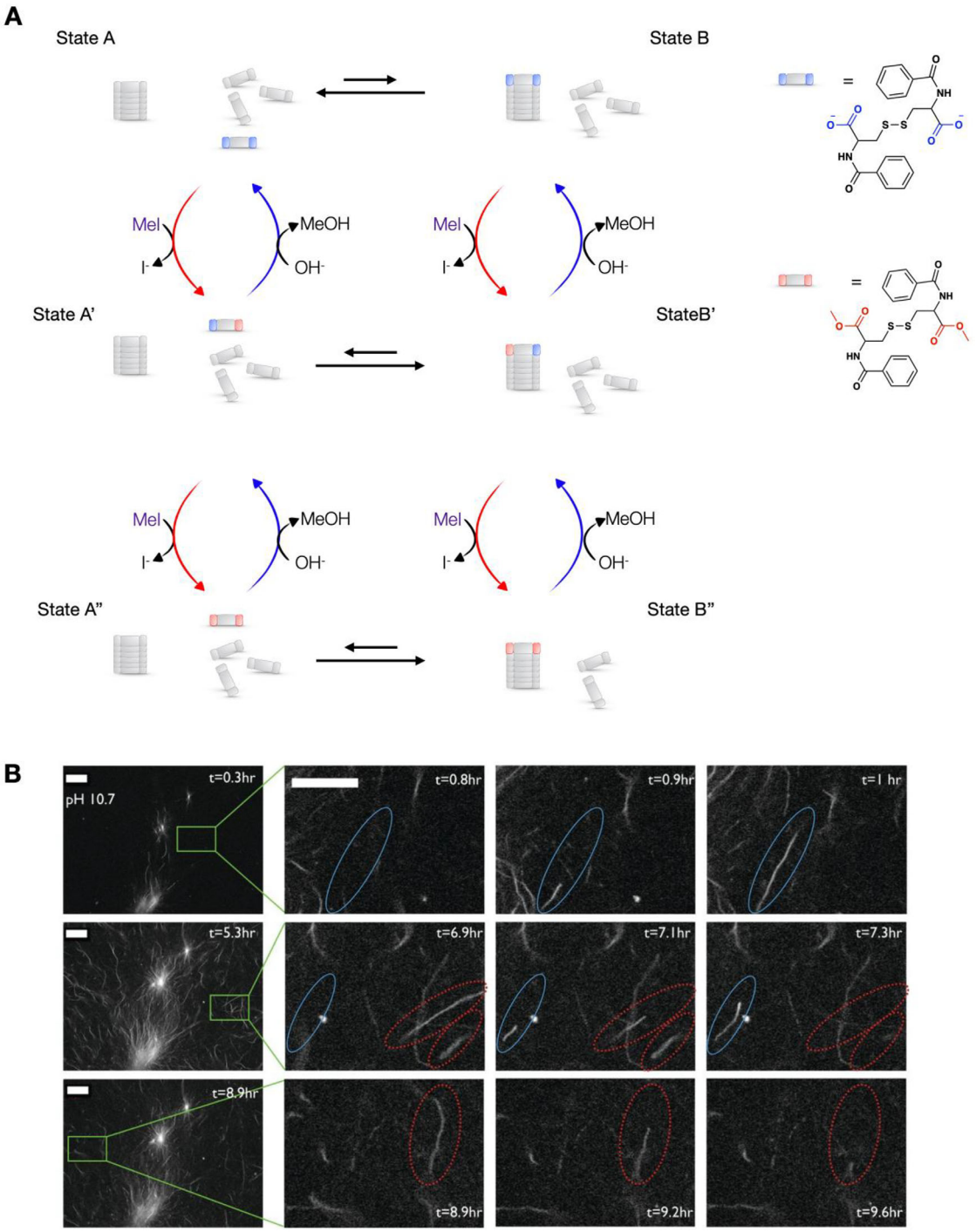

FIGURE 6 | Chemically fueled dynamic assemblies. (A) MeI-driven assembly and disassembly of the small molecule dibenzoyl-L-cysteine (DBC) into fibers. Molecular design of building blocks. (B) Confocal micrographs over time show distinct fiber growth, shrinkage, and overlapping periods during a reaction cycle. Blue circles indicate growing fibers, and red circles indicate shrinking fibers. Scale bar = 10 μm. Reprinted with permission [46].

4.2.2 | Chemically Fueled Supramolecular Materials

The dynamic behavior of chemically fueled assemblies opens the door to designing supramolecular materials endowed with properties unique to their non-equilibrium nature. First and foremost is their dependence on fuel. Because chemically fueled materials require fuel that depletes, they are transient, and the amount of fuel can control their lifetime. This temporal control has been explored for several materials like transient gels [46, 96], emulsions [95, 97, 124, 130, 131], and optical devices [139–141].

One possible application of such materials is to deliver molecules with temporal control. Supramolecular materials have been demonstrated to be promising drug-delivery platforms, and their combination with chemical reaction cycles enables spatiotemporal release of molecules, such as drugs [130, 142]. For example, one study used the kinetic feature of the constant

16163028, 2026, 68, Downloaded from https://advanced.onlinelibrary.wiley.com/doi/10.1002/adfm.77237, Wiley Online Library on [17/11/2026]. See the Terms and Conditions (https://onlinelibrary.wiley.com/terms-and-conditions) on Wiley Online Library for rules of use; OA articles are governed by the applicable Creative Commons License

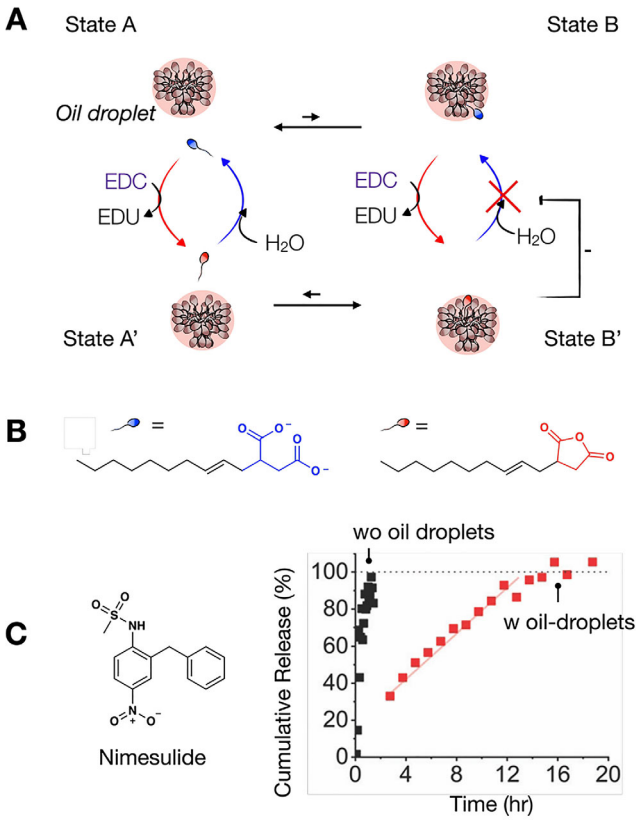

FIGURE 7 | Chemically Fueled Supramolecular Materials I. (A–C) Fuel-driven oil droplets as a drug delivery platform. (A) Carbodiimide-driven formation of oil droplets. The activated assembled, activated catalyst (state B') does not deactivate as it is phase separated from the water needed for hydrolysis. This negative feedback results in a zero-order-kinetic decay profile for the oil droplets (B). Molecular structure of the catalyst and the activated catalyst. (C) Cumulative release of Nimesulide from the oil droplets against time with (red markers) and without (black markers) droplets. As the oil droplets hydrolyze with zero-order kinetics, the drug is also released with linear kinetics. Adapted with permission from the authors.

zero-order decay of carbodiimide-driven oil droplets to uptake and subsequently deliver the hydrophobic anti-inflammatory drug nimesulide and the hydrophobic calcium channel blocker nitrendipine (Figure 7A–C) [130]. Specifically, the catalyst in its activated state can phase separate into oil droplets with other activated catalysts. In these oil droplets, the activated catalyst is physically separated from the water required for its deactivation, thereby inhibiting deactivation via this pathway. Deactivation can thus only occur through the fraction that remains in solution, which is equal to the oil's solubility and constant. Thus, the hydrolysis occurs through zero-order (constant) kinetics equal to the deactivation rate constant multiplied by the oil's solubility. This self-protection mechanism thus result in characteristic linear deactivation kinetics.

In another example, the authors used the transient character of ATP-driven DNA-based coacervate droplets to uptake and release functionalized micron-scale colloids as well as functional DNA polymers [142]. These examples showcase that chemical energy, when coupled to a molecular assembly process, can be used to achieve an uptake and release function. Another unique property of these materials is that, due to their dynamic nature, they can be self-healing. For example, a recent study described carbodiimide-driven fibers that build up a hydrogel (Figure 8A–C) [123]. Under continuous fuel supply, the hydrogel can self-heal when damaged. Self-healing occurs as the deactivated catalyst from the solution activates, attaches to the fiber end caps, and regenerates the fibrous structure.

4.2.3 | Sustain Dissipative Structures

Dissipative structures are dynamic, ordered structures that can only exist in a non-equilibrium steady state, thus requiring continuous energy exchange to maintain their organized state. These states can be structured and stable over time. However, when feedback is involved, these states can also become unstable and rhythmically oscillate between stability and unstability [143]. When a reactor is continuously supplied with reagents, a steady state is expected; when this steady state spontaneously becomes unstable and begins to oscillate, we speak of a temporal dissipative structure. Similarly, when the solution becomes inhomogeneous, spatial dissipative structures emerge, often referred to as Turing patterns [144].

Chemically fueled assemblies can become dissipative structures when continuously supplied with fuel. Although continuous fueling can be challenging, it has recently been shown that a redox-driven assembly of perylene diimide (PDI) can spontaneously begin oscillating when supplied with a steady influx of fuel (Figure 9) [122]. The system is kept out of equilibrium by a constant fuel supply of oxidant O_2 and reductant $Na_2S_2O_4$. Oxidation leads to the activation of PDI^{2-} (state A) to PDI (Figure 9A, state A″), negating the two negative charges, which drive self-assembly into nanofibers that subsequently organize into micrometer-sized colloids (state B″). Reduction led to the deactivation of PDI^{2-} which drives disassembly (state B). On paper, such a system should result in a steady state in which assemblies are both growing and shrinking. However, the opposite was true. The solution oscillated between periods of growth and shrinkage (Figure 9C). This oscillation resulted from the assembled PDI exerting positive feedback on its own growth. At the same time, the fiber stacks exhibited negative feedback on their deactivation due to size-dependent depolymerization. Thus, because of nonlinearity in assembly growth and a feedback mechanism by which the assembly affects its chemical reaction cycle, the solution begins to oscillate. The beauty of this system lies in the interplay of positive and negative feedback on the chemical reaction, resulting in autonomous oscillatory behavior of colloid formation and degradation.

In another rare example of oscillating assemblies in response to a steady fuel flux, the authors coupled the redox-driven catalyst activation and deactivation with a micellar assembly process that exerts positive feedback on catalyst activation and subsequently positive feedback on catalyst deactivation [145]. The delicate interplay between self-amplification and self-destruction feedback results in oscillatory behavior in the formation and degradation of activated catalysts under a constant fuel supply. The oscillations in this system are strongly coupled to the

16163028, 2026, 68, Downloaded from https://advanced.onlinelibrary.wiley.com/doi/10.1002/adfm.77237, Wiley Online Library on [17/11/2026]. See the Terms and Conditions (https://onlinelibrary.wiley.com/terms-and-conditions) on Wiley Online Library for rules of use; OA articles are governed by the applicable Creative Commons License

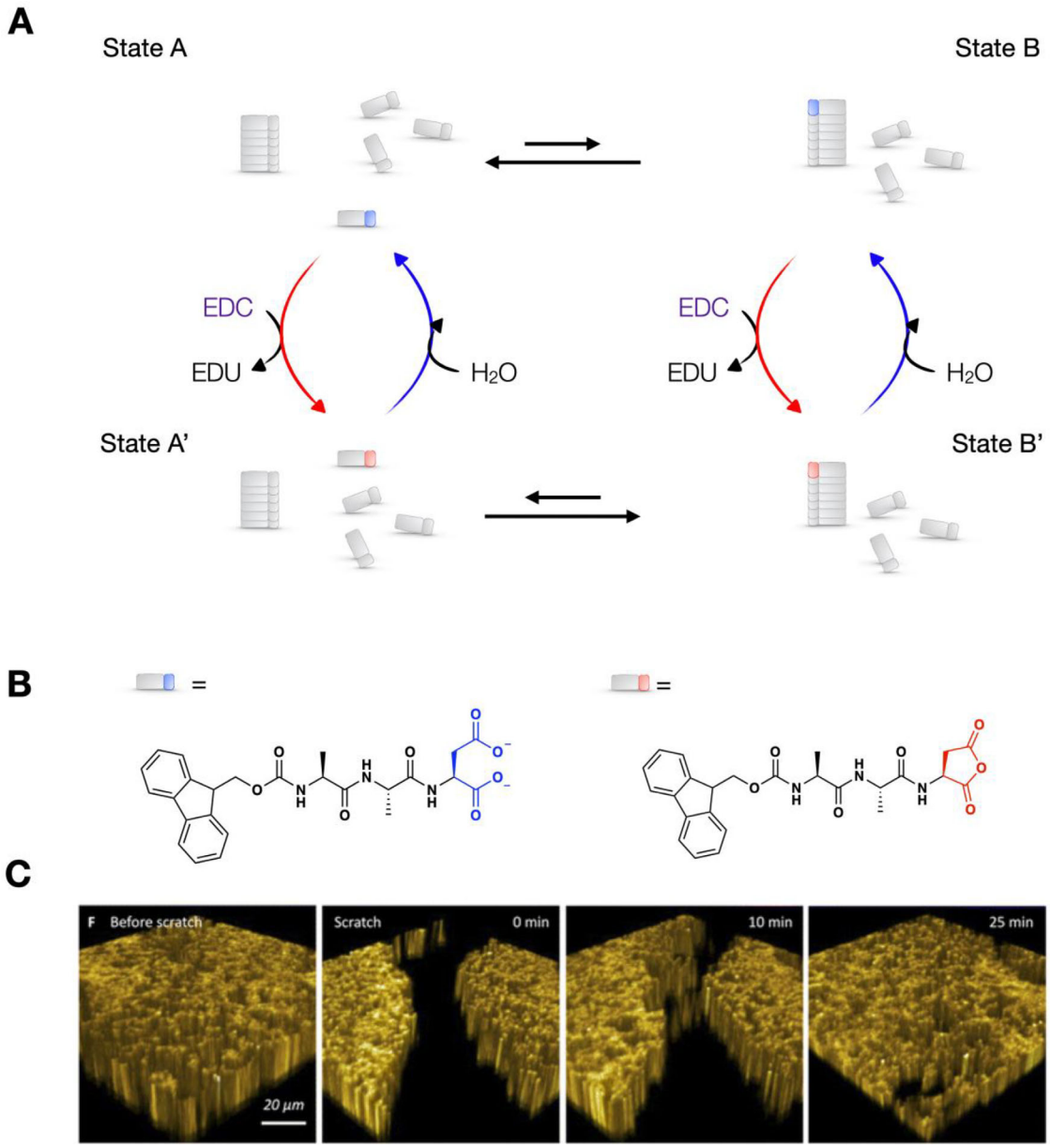

FIGURE 8 | Chemically fueled supramolecular materials II. (A–C) Fuel-driven self-healing fibers. (A) Carbodiimide-driven assembly and disassembly of the Fmoc-AAD-peptide into fibers. (B) Molecular structure of the non-activated and activated catalyst Fmoc-AAD. (C) 3D reconstruction of confocal fluorescence microscopy data shows the self-healing of EDC-fueled Fmoc-AAD fiber network over the course of 25 min after performing a scratch. Adapted with permission from the authors.

concentration of the constant fuel flux and can be tuned by the rate of oxidation and reduction.

In addition to oscillations, feedback on the chemical activation and deactivation of the catalyst during assembly can give rise to bistability, in which a steady state results in two stable states (Figure 10A–C) [135]. The reported system involved EDC-fueled crystallization in which a Boc-aspartic acid catalyst (state A) catalyzes EDC-to-EDU conversion and thereby activates the anhydride (state A'), which crystallizes above a critical anhydride concentration (state B'). The crystals exert negative feedback on their catalyst (state B') deactivation, i.e., they protect their building blocks from deactivation. Thus, the deactivation only occurs on the activated state that is not assembled (state A'). As a result, deactivation is severely slowed down when crystals are present. Because the crystallization of state A' requires passing a threshold nucleation concentration, it is possible to create two stable steady states, one in which crystals were never present and one in which crystallization occurred (for example, by adding a seed). Once the crystals are present, the feedback mechanism slows deactivation, thereby increasing the concentration of the activated state and allowing the crystals to continue forming. This system demonstrates that chemical energy can be harnessed to construct a bistable system capable of storing volatile memory.

Recently, a spatially dissipative structure was formed in a continuously fueled microreactor, in which a carbodiimide-driven reaction cycle is coupled to droplet formation. Upon reaction with

16163028, 2026, 68, Downloaded from https://advanced.onlinelibrary.wiley.com/doi/10.1002/adfm.77237, Wiley Online Library on [17/11/2026]. See the Terms and Conditions (https://onlinelibrary.wiley.com/terms-and-conditions) on Wiley Online Library for rules of use; OA articles are governed by the applicable Creative Commons License

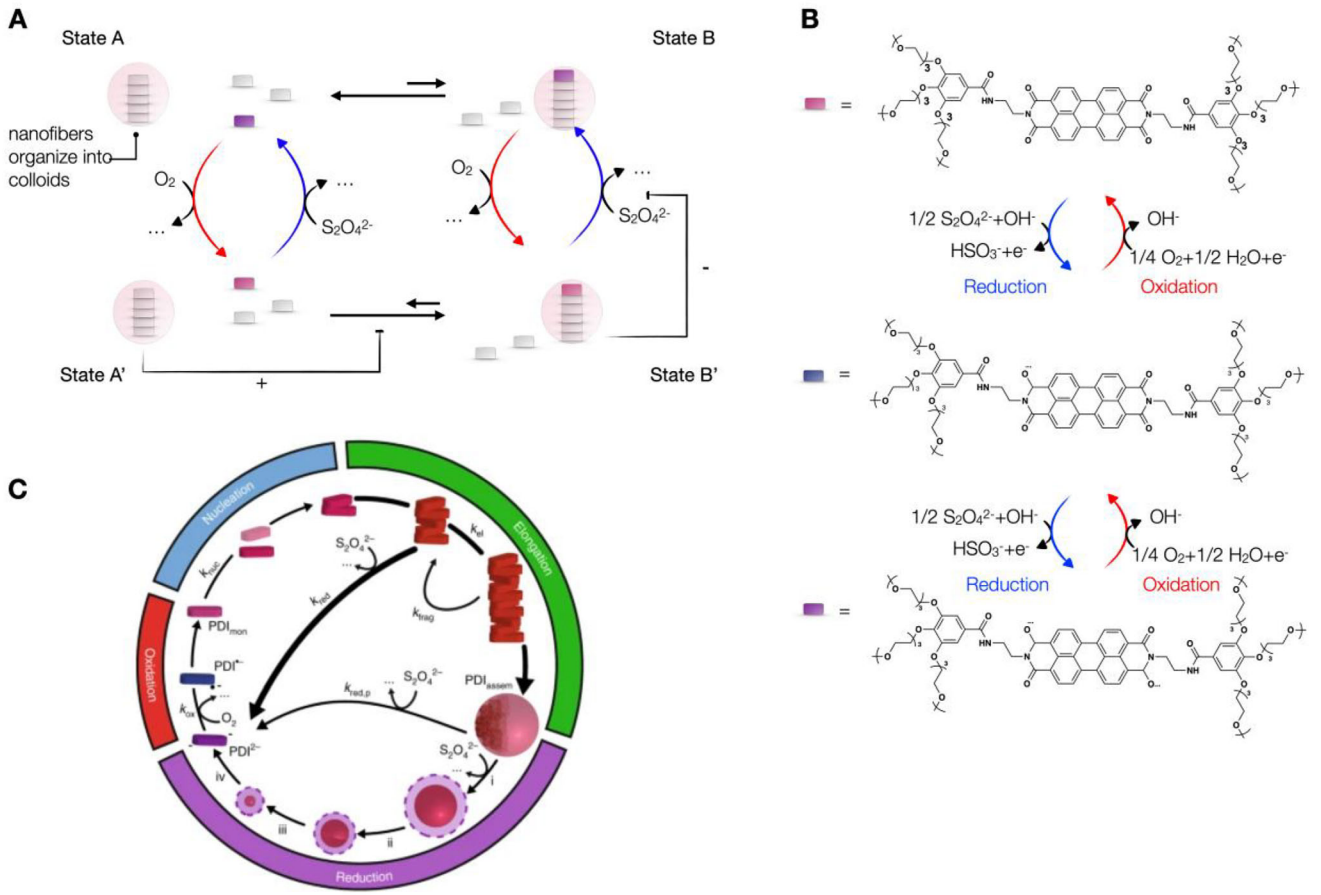

FIGURE 9 | Oscillatory behavior through feedback mechanisms. (A) Oxidation-reduction-driven formation of nanofibers. The nanofibers have negative feedback on the deactivation of the activated catalyst and a positive feedback on their formation. We can describe the single catalyst perspective with a 2 × 2-state model. (B) Molecular structure and chemical reaction cycle of the PDI oxidation and reduction. Upon addition of Na_2S_2O PDI reduces to PDI^{2-}. The first radical anion $PDI^{\bullet -}$ and then to the neutral PDI forms through spontaneous oxidation in air. (C) After one redox cycle, i.e., the reduction to PDI^{2-} and oxidation to PDI_{mon}, PDI_{mon} grows via a cooperative polymerization mechanism with nucleation k_{nuc}, elongation $k_{el,}$ and fragmentation k_{frag} constants. A size-dependent reduction rate for PDI_{assem} ($k_{red,p}$) characterizes the system. Adapted with permission [122].

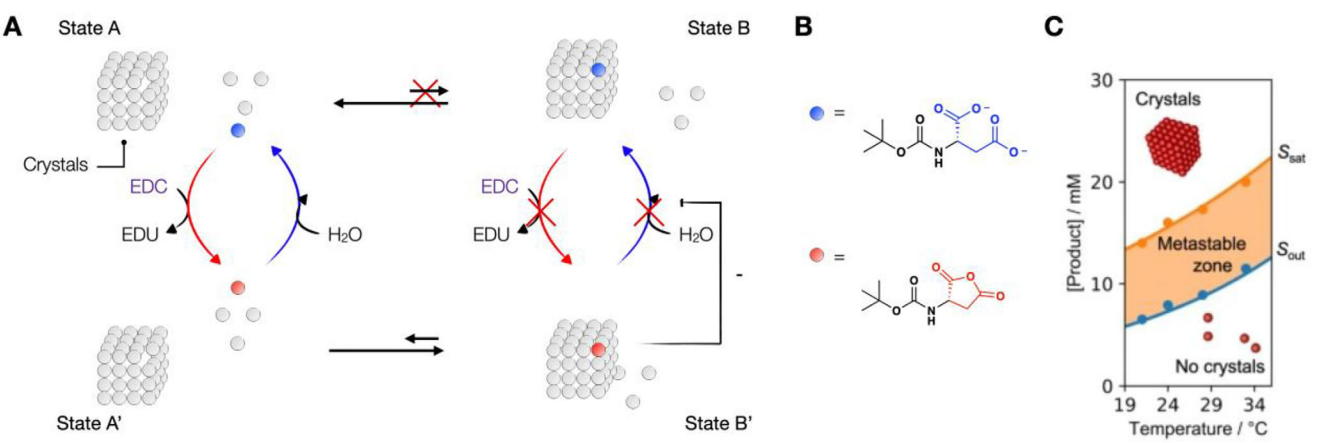

FIGURE 10 | Chemically fueled crystal formation opens the door for bistability capable of storing volatile memory. (A) Carbodiimide-driven formation of crystals. The crystals have negative feedback on the deactivation of the activated catalyst. We can describe the single-catalyst perspective using a 2 × 2 state model. (B) Molecular structure of the catalyst and the activated catalyst. (C) The phase diagram of crystallization of the activated catalyst. In the metastable zone, a solution without or with crystals can exist. Adapted with permission.

16163028, 2026, 68, Downloaded from https://advanced.onlinelibrary.wiley.com/doi/10.1002/adfm.77237, Wiley Online Library on [17/11/2026]. See the Terms and Conditions (https://onlinelibrary.wiley.com/terms-and-conditions) on Wiley Online Library for rules of use; OA articles are governed by the applicable Creative Commons License

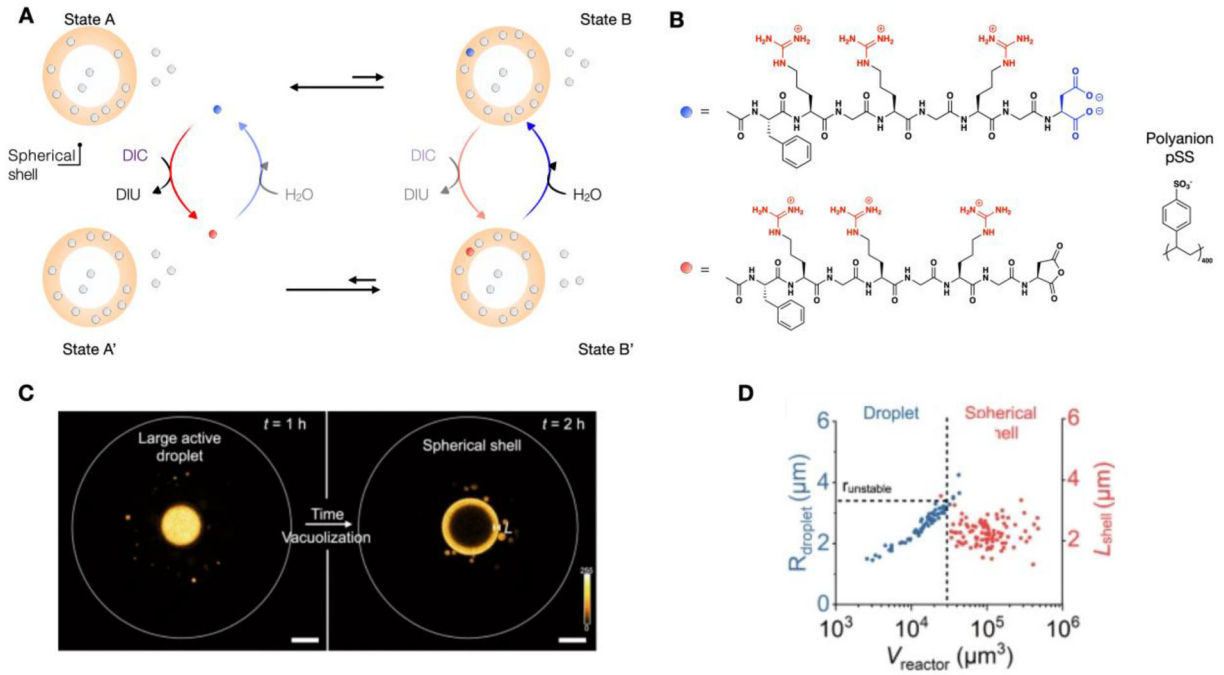

FIGURE 11 | Chemical fuel sustains and maintains the dissipative structure of spherical shells. (A) Carbodiimide-driven formation of spherical shells. We can describe the single catalyst perspective with a 2 × 2 state model. (B) Molecular structure of the catalyst, the activated catalyst and the polyanion. (C) Time-lapsed micrographs of surfactant-stabilized microfluidic droplets (microreactors, grey outline) in steady state. The microfluidic droplet contains 10 mM non-activated catalyst (blue in B), 5 mM pSS, and 0.1 μM sulforhodamine B in 200 mM MES buffer at pH 5.3. The microfluidic droplets are embedded in a fluorinated oil, which contains 0.5 M DIC (fuel) to sustain the microreactor at a fuel concentration of 8.4 mM. The image for 10 min is a Z-projection of the microreactor, and all other images are from one Z-plane. The scale bar is 10 μm, and the color scale is given next to the images. (D) The radius of the active droplet (blue) and the shell thickness L of the active shell (red) for different microreactors. Spherical shells had a similar thickness L_{shell}, which was within the range of $r_{unstable}$. Experiments are performed in triplicate (N = 3). (C,D) Adapted and reprinted with permission from the authors.

fuel, the catalyst (state A) is activated (state A') (Figure 11A,B). The activated state was designed to phase separate and form droplets (state B'). The activated state could deactivate through hydrolysis, either inside the droplets (state B') or outside of the droplets (state A'). Under continuous fuel supply, the reactor produces droplets that fuse and eventually form one large active droplet (Figure 11C). However, when the large droplet is larger than a critical radius, it spontaneously transitions into a spherical shell of liquid droplet material (Figure 11D). From a thermodynamic standpoint, this is surprising—the spherical shell has more than doubled its surface area, which is very unfavorable. The mechanism behind the transition involves the formation of a reaction-diffusion pattern. Because the droplet itself consumes some fuel, it becomes depleted of fuel. Thus, the core cannot re-activate the catalyst, which must leave the droplet to be reactivated. This efflux of deactivated droplet material and the influx of activated droplet material imply that the shell of the droplet receives material while the core is decaying. Then, the droplet is too large, resulting in a transition in which the droplet core dissolves, leaving only the shell.

4.3 | Chemically Fueled Molecules With Multiple Catalytic Sites

We described examples in which chemical reaction cycles are coupled to intramolecular and intermolecular supramolecular processes that are regulated by single-point or double-point activation of molecules. In this section, we describe the implications when the chemical reaction cycle regulates intramolecular and intermolecular interactions through multipoint activation of molecules. If polymers or nanoparticles are used as backbone motifs, they can be designed to bear multiple catalytic sites on which the fuel can act. Those multipoint catalysts are designed to interact with one another via noncovalent interactions. Intramolecular interactions drive folding, whereas intermolecular interactions drive assembly or cross-linking. Compared to single-point catalysts, for which we distinguish between activated states A', B', and non-activated states A, B, we need to distinguish between n x 2 states, in which n describes the number of possible activated states. Besides, when these states can assemble with m building blocks, we have to consider n x m possible states for multipoint catalysts (Figure 2C,D). Thus, the catalyst is not switched on and off sharply. Moreover, the picture becomes more complex when there are multiple assembly states in between fully activated and deactivated, i.e., activation of some catalytic sites can already lead to partial folding or assembly of those catalysts. Put differently, for these multipoint catalysts, the complete kinetic description becomes much more complex than for the 4-state models described above. Ideally, the catalyst in its fully non-activated state does not assemble, i.e., the equilibrium position for state nA to state nB lies to the left. Upon stepwise activation, the partly activated catalyst is more likely to assemble, i.e., the equilibrium position lies to the right.

16163028, 2026, 68, Downloaded from https://advanced.onlinelibrary.wiley.com/doi/10.1002/adfm.77237, Wiley Online Library on [17/11/2026]. See the Terms and Conditions (https://onlinelibrary.wiley.com/terms-and-conditions) on Wiley Online Library for rules of use; OA articles are governed by the applicable Creative Commons License

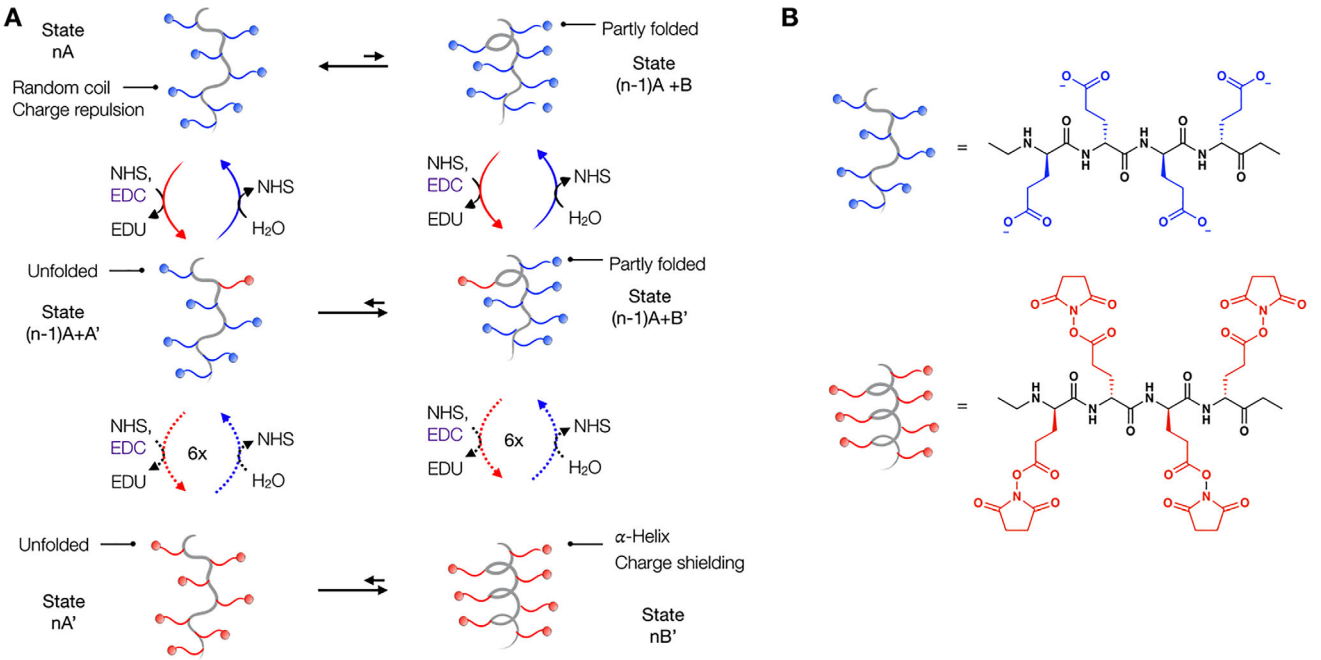

FIGURE 12 | Intramolecular structural transitions by multipoint activation/deactivation. (A) A carbodiimide-driven folding of poly-L-glutamic acid (PLG) into coiled helices upon multipoint activation. (B) Molecular structure of the poly-L-glutamic acid (PLG) before and after NHS+EDC activation. Adapted with permission [146].

There is no interaction in this scenario when no chemical fuel is present. When fuel is present, the mA' and mB' equilibrium is populated, leading to the intra-and/or intermolecular interaction of the catalyst molecules. The following section presents selected examples of chemically fueled multipoint catalysts and explains their potential for the design of spatiotemporally controllable materials.

4.3.1 | Chemically Fueled Intramolecular Transitions Controlled by Multipoint Activation

Similar to protein folding, in which multiple side chains undergo supramolecular interaction, synthetic molecules can be designed to fold not through multipoint activation. For example, carbodiimide-driven folding of poly-L-glutamic acid (PLG) into coiled helices has been reported (Figure 12) [146]. The PLG molecule (state nA) connects multiple catalytic carboxylate sites and adopts a random coil conformation in aqueous conditions. In the presence of the nucleophile N-hydroxysuccinimide (NHS), the EDC-fuel activates the carboxylate catalytic sites to the corresponding NHS-ester (state (n-m)AmA'), which drives folding into an α-helix due to charge-negation. Reintroduction of these charges upon deactivation results in a partially unfolding (state (n-m)A) if the majority of catalytic sites are still activated. Complete deactivation of the PLG returns the PLG to its unfolded random coil state nA. In such systems, continuous fuel consumption enables the maintenance of high-energy folded states. Coupling this high-energy folded state to a specific material function, e.g., catalysis, uptake of molecules, enables spatiotemporal control over material functions. Similarly, carbodiimide-driven deswelling and swelling of micron-sized microgels comprised of a crosslinked poly(2,2,2,-tri-fluoroethyl methacrylate core (PTFEMA) and a poly(methacrylic acid) (PMAA)-based shell have been reported [79]. Here, stepwise activation drives an intramolecular structural transition of the microgel that results in deswelling. Stepwise deactivation drives the partial reswelling of the microgel [79].

4.3.2 | Chemically Fueled Nanoparticle and Polymer Assemblies can be Dynamic

Similar to molecular self-assembly, nanoparticles and polymers can self-assemble. Coupling polymer assembly/disassembly with a chemical-fueled reaction cycle enables kinetically controlled assembly and disassembly of nanoparticles and polymers. For example, carbodiimide-driven assembly and disassembly of photoluminescent Si-nanoparticles (SiNC) have been reported (Figure 13) [147]. The SiNCs (state nA) bear multiple catalytic carboxylate sites on their surface and are overall negatively thereby hindering their self-assembly. In the presence of the nucleophile N-Hydroxysuccinimid (NHS), the EDC-fuel activates the carboxylate catalytic sites to the corresponding NHS-ester, which negates the negative surface charges and drives the assembly of the SiNCs. Charge introduction upon deactivation leads to partial disassembly of nanoparticles when most catalytic sites remain active. Complete deactivation of all catalytic sites drives the disassembly of nanoparticles nA. In such systems, continuous fuel consumption enables the maintenance of high-energy assembled states. Coupling this high-energy assembled state to a specific material function; here, the carbodiimide-driven SiNC assembly delays the uptake by mammalian cells. Another example [148]. reports the allylic substitution-driven disassembly of polymer micelles that is used to uptake and release the hydrophobic dye molecule Nile Red. The inverted

16163028, 2026, 68, Downloaded from https://advanced.onlinelibrary.wiley.com/doi/10.1002/adfm.77237, Wiley Online Library on [17/11/2026]. See the Terms and Conditions (https://onlinelibrary.wiley.com/terms-and-conditions) on Wiley Online Library for rules of use; OA articles are governed by the applicable Creative Commons License

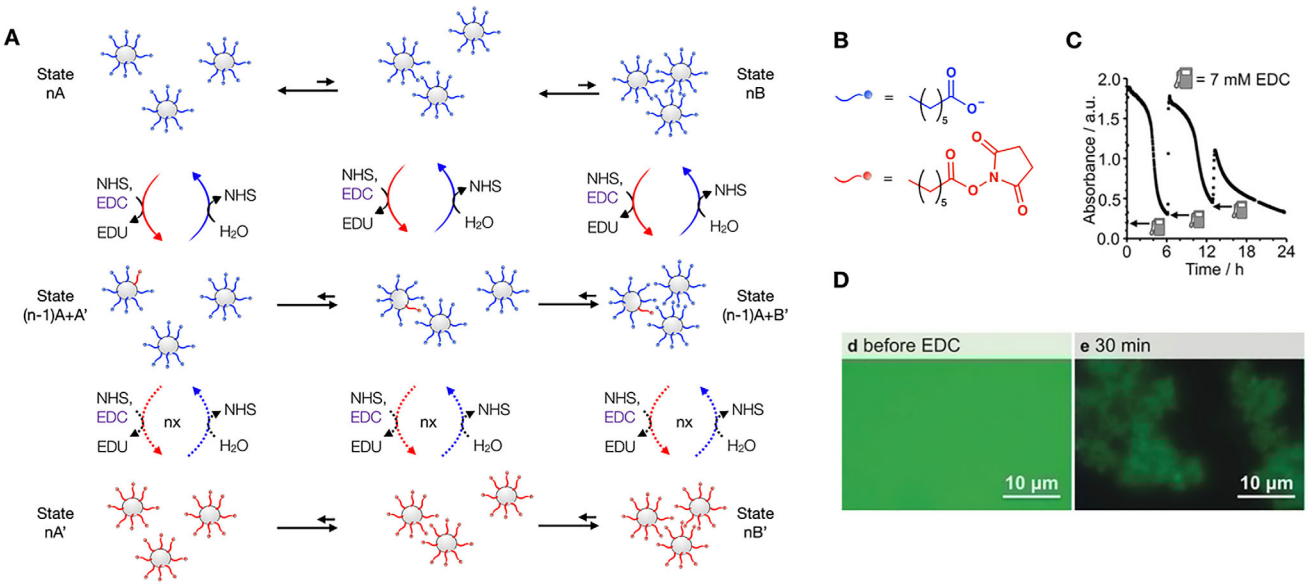

FIGURE 13 | Assembly and disassembly of Si-nanoparticles by multipoint activation and deactivation. (A) Carbodiimide-driven assembly and disassembly of nanoparticles. (B) Molecular structure of the functional groups before and after NHS+EDC activation. (C) Absorbance at 500 nm when 7 mM EDC is added three times consecutively to the same SiNC solution. (D) Fluorescent micrographs of the intrinsically fluorescent SiNCs were acquired before and 30 min after the addition of 7 mM EDC. (C, D) Reprinted with permission from the authors.

approach, i.e., charge negation and subsequent charge introduction, was used to drive carbodiimide-fueled self-assembly and disassembly of block-copolymer micelles [134]. Those chemical-fuel-driven block-copolymer micelles have been used to catalyze a Diels-Alder reaction through the up concentration of diene and dienophile. Remarkably, the reaction yield can be controlled with the amount of fuel. In another example, carbodiimide-driven block copolymers catalyze anthracene dimerization [149]. Besides these polymer catalyst examples [125, 134, 148–150], the strategy of chemically fueled charge negation has been widely exploited to achieve chemical fuel-driven assembly and disassembly of colloidal [47] or nanoparticle [60, 151, 152], catalysts, and recently also for molecular cages [153] that connect multiple catalytic sites.

4.3.3 | Chemically-Fueled Crosslinking to Perform Work

Coupling a chemical reaction cycle to molecules, such as polymers, nanoparticles, and colloidal particles, enables covalent crosslinking that renders them stimuli-responsive and thereby temporally controls their properties, e.g., polymer stiffness [81, 82, 154–158]. For example, carbodiimide-driven covalent crosslinking of polymers has been reported to form a hydrogel (Figure 14) [81, 158]. In more detail, copolymers of acrylamide and acrylic acid carry multiple carboxylate catalytic sites (state nA), which catalyze the EDC-to-EDU conversion while activating the anhydride states (state (n-m)A mA'). Intermolecular anhydride formation between different copolymer strands covalently crosslinks copolymer strands (state (n-m)A,mA') and builds a hydrogel. Due to the covalent crosslinking, the hydrogel exhibits higher storage moduli compared to supramolecular hydrogels that are only held together by non-covalent interactions. Hydrolysis deactivates the copolymer catalyst (state (n-m)AmA'). When all fuel is consumed and the majority of catalytic sites are deactivated, the hydrogel dissolves back into the aqueous copolymer solution (state nA). The cycle can be reinitiated. This approach yields transient covalently crosslinked polymer hydrogels. A follow-up study [82] reported the influence of polymer design, temperature, and fuel concentration on the mechanical properties of transient polymers. The study shows that fuel concentration tunes the gel's lifetime and storage modulus. High fuel concentrations lead to more covalent anhydride crosslinks, thereby increasing storage moduli and polymer network lifetimes. Similarly, temperature affects network lifetimes but has a small effect on the storage moduli. These findings inform the design of tunable, on-demand polymer gels and networks.

The carbodiimide-driven approach has been exploited in further studies to regulate material properties [80, 154–156, 159]. For example, carbodiimide-driven polymer hydrogels have been exploited as transient reservoirs for the controlled formation and free release of pharmaceutical crystals, e.g., carbamazepine [156]. Another study reports a carbodiimide-driven soft hydrogel actuator that shows autonomous self-resetting behavior [80]. Coupling non-equilibrium chemical reaction cycles with polymer materials also enables time-controlled adhesion and pattern formation in polymer hydrogels [154]. Besides synthetic polymers, hydrogel formation by redox-driven covalently crosslinking unfolded proteins has been reported as well [160].

5 | Conclusion and Challenges Ahead

The literature reviewed in this article shows that coupling the non-equilibrium chemical reaction cycle to supramolecular processes provides a platform for kinetically regulating distinct properties and functions at the nano-, micro-, and millimeter scales. For instance, we can kinetically regulate optical properties, molecular release, catalysis, and conformational structures across

16163028, 2026, 68, Downloaded from https://advanced.onlinelibrary.wiley.com/doi/10.1002/adfm.77237, Wiley Online Library on [17/11/2026]. See the Terms and Conditions (https://onlinelibrary.wiley.com/terms-and-conditions) on Wiley Online Library for rules of use; OA articles are governed by the applicable Creative Commons License

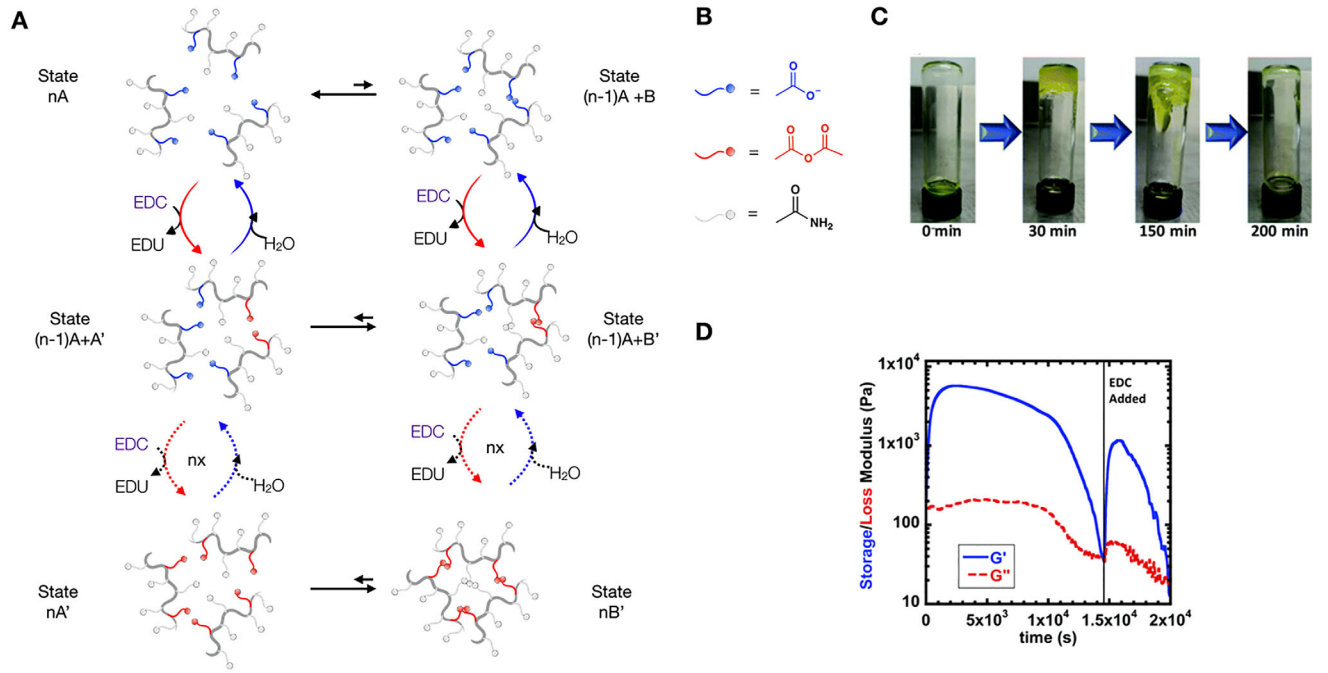

FIGURE 14 | Intermolecular crosslinking by multipoint activation and deactivation. (A) A carbodiimide-driven covalent crosslinking of polymers. (B) Molecular structure of the functional groups before and after EDC activation. (C) Time-lapse photographs of inverted vial tests for poly(Am85-r-AA15) upon treatment with EDC (conditions: 0.8 mL, 0.5 g mL^{-1} polymer, 0.5 eq. EDC). (D) Rheology for the poly(AM85-r-AA15) at 10 Hz with repetitive addition of EDC at 4°C. (C, D) Reprinted with permission [81].

various length scales. Moreover, this approach enables chemo-mechanical coupling in synthetic systems, i.e., systems in which chemical energy is converted into mechanical motion. Leveraging this basic concept, along with the delivered design strategies, provides scientists with a tool for designing new functional, adaptive, autonomous, chemically powered materials and machines, e.g., nano- and micrometer-sized machines such as a synthetic cell with a synthetic flagellum in future work. We showed that chemically fueled single-point catalysts can be described by a four-state (2 × 2) model, which can be extended to a four-state (2 × 2) model to a 2xn-state model to describe the assembly of single-point catalysts and to an nx2-and an nxm-state model to describe multipoint catalysts.

However, we believe that the full potential of this approach has not yet been realized. For instance, there are no chemically fueled supramolecular micro walkers like the ATP-fueled kinesin walker [2], supramolecular fibers that show treadmilling like the actin filaments [5–7] or supramolecular muscles that contract and expand like human muscles [161]. A technical complication that requires further attention is the accumulation of waste in these assemblies, particularly when a supramolecular system is maintained in a steady state, and fuel is continuously supplied. Some systems address this challenge, but more solutions are required. Moreover, so far, we can only describe the underlying kinetic rate constants and binding constants well for single-point catalysts using the four-state model, but only partially on the assembly scale. While such theory and calculations have been extremely powerful for predicting the performance of molecules, applying the four-state (2 × 2) model, these calculations become increasingly complex with higher-state models. Future work needs to address the technical challenges that currently hinder our ability to fully describe the dynamic systems of single-point and multipoint catalysts at the assembly scale.

Nevertheless, with the design strategies we developed for coupling the non-equilibrium chemical-fueled reaction cycle to supramolecular processes across different length scales, the analytical techniques we developed to analyze these systems, and the development of theory and computation to predict exciting new behavior, we are developing the tools to create new functional, autonomous, adaptive materials and systems. For instance, to achieve micro robots, we can couple single-molecule-scale phenomena (e.g., directional rotation) to the micro- to millimeter-length scale. Besides, we can use this approach to develop biocompatible chemically fueled therapeutics or further develop the chemically fueled cargo-delivery approach to achieve kinetically controlled small-molecule encapsulation or release for therapeutics or wastewater treatment (e.g., transient cages, micelles). We envision that, as we move toward applications, non-equilibrium systems can be useful across a wide range of applications, including biomaterials, drug delivery, and sensors.

Author Contributions

J.B. and B.A.K.K. conceived the research and wrote the manuscript.

Acknowledgements

The BoekhovenLab is grateful for continuous support by the TUM. This research was conducted within the Max Planck School Matter to Life, supported by the Dieter Schwarz Foundation in collaboration with the

16163028, 2026, 68, Downloaded from https://advanced.onlinelibrary.wiley.com/doi/10.1002/adfm.77237, Wiley Online Library on [17/11/2026]. See the Terms and Conditions (https://onlinelibrary.wiley.com/terms-and-conditions) on Wiley Online Library for rules of use; OA articles are governed by the applicable Creative Commons License

Max Planck Society. B.A.K.K. is grateful for a Kekulé-Stipendium by the Verbandes der Chemischen Industrie.

Open access funding enabled and organized by Projekt DEAL.

Conflicts of Interest

The authors declare no conflicts of interest.

Data Availability Statement

Data sharing not applicable to this article as no datasets were generated or analysed during the current study.

References

1. J. V. Moller, P. Nissen, T. L. Sorensen, and M. le Maire, "Transport Mechanism of the Sarcoplasmic Reticulum Ca^{2+}-ATPase Pump," *Current Opinion in Structural Biology* 15 (2005): 387–393, https://doi.org/10.1016/j.sbi.2005.06.005.

2. A. Marx, A. Hoenger, and E. Mandelkow, "Structures of Kinesin Motor Proteins," *Cell Motility* 66 (2009): 958–966, https://doi.org/10.1002/cm.20392.

3. I. Rayment, H. M. Holden, M. Whittaker, et al., "Structure of the Actin-Myosin Complex and Its Implications for Muscle Contraction," *Science* 261 (1993): 58–65, https://doi.org/10.1126/science.8316858.

4. H. L. Sweeney and E. L. F. Holzbaur, "Motor Proteins," *Cold Spring Harbor Perspectives in Biology* 10 (2018): a021931.

5. B. Alberts, A. Johnson, J. Lewis, M. Raff, K. Roberts, and P. Walter, *Molecular Biology of the Cell*, 4th ed. (Garland Science, 2002).

6. H. H. Katkar, A. Davtyan, A. E. P. Durumeric, et al., "Insights into the Cooperative Nature of ATP Hydrolysis in Actin Filaments," *Biophysical Journal* 115 (2018): 1589–1602, https://doi.org/10.1016/j.bpj.2018.08.034.

7. G. M. Cooper, *The Cell: A Molecular Approach*, 2nd ed. (Sinauer Associates, 2000).

8. D. Ortega and M. Beeby, "How Did the Archaellum Get Its Rotation?," *Frontiers in Microbiology* 12 (2021): 803720, https://doi.org/10.3389/fmicb.2021.803720.

9. S. Iwata, Y. Kinosita, N. Uchida, D. Nakane, and T. Nishizaka, "Motor Torque Measurement of Halobacterium Salinarum Archaellar Suggests a General Model for ATP-driven Rotary Motors," *Communications Biology* 2 (2019): 199, https://doi.org/10.1038/s42003-019-0422-6.

10. Y. Deng, G. Long, Y. Zhang, et al., "Photo-responsive Functional Materials Based on Light-Driven Molecular Motors," *Light: Science & Applications* 13 (2024): 63, https://doi.org/10.1038/s41377-024-01391-8.

11. M. Weißenfels, J. Gemen, and R. Klajn, "Dissipative Self-Assembly: Fueling with Chemicals versus Light," *Chemistry* 7 (2021): 23–37, https://doi.org/10.1016/j.chempr.2020.11.025.

12. C. Chen and Z. Guan, "Precise Control of Dissipative Self-Assembly by Light and Electricity," *Chemistry–A European Journal* 29 (2023): 202300347.

13. D. Barpuzary, P. J. Hurst, J. P. Patterson, and Z. Guan, "Waste-Free Fully Electrically Fueled Dissipative Self-Assembly System," *Journal of the American Chemical Society* 145 (2023): 3727–3735, https://doi.org/10.1021/jacs.2c13140.

14. S. Selmani, E. Schwartz, J. T. Mulvey, et al., "Electrically Fueled Active Supramolecular Materials," *Journal of the American Chemical Society* 144 (2022): 7844–7851, https://doi.org/10.1021/jacs.2c01884.

15. X.-F. Hou, X. Chen, J.-H. Wei, Y. Xu, X.-M. Chen, and Q. Li, "Peptide-Based Antibacterial Nanoplatforms: Design Principles, Stimuli-Regulated Behaviors, and Applications," *Responsive Materials* 1 (2023): 20230016.

16. J. Boekhoven, A. M. Brizard, K. N. K. Kowlgi, G. J. M. Koper, R. Eelkema, and J. H. van Esch, "Dissipative Self-Assembly of a Molecular Gelator by Using a Chemical Fuel," *Angewandte Chemie* 122 (2010): 4935–4938, https://doi.org/10.1002/ange.201001511.

17. D. Zala, U. Schlattner, T. Desvignes, et al., "The Advantage of Channeling Nucleotides for Very Processive Functions," *F1000Research* 6 (2017): 724.

18. J. Akola and R. O. Jones, "ATP Hydrolysis in Water – A Density Functional Study," *The Journal of Physical Chemistry B* 107 (2003): 11774–11783, https://doi.org/10.1021/jp035538g.

19. C. T. Walsh, B. P. Tu, and Y. Tang, "Eight Kinetically Stable but Thermodynamically Activated Molecules That Power Cell Metabolism," *Chemical Reviews* 118 (2018): 1460–1494, https://doi.org/10.1021/acs.chemrev.7b00510.

20. M. Brini and E. Carafoli, "The Plasma Membrane Ca2+ ATPase and the Plasma Membrane Sodium Calcium Exchanger Cooperate in the Regulation of Cell Calcium," *Cold Spring Harbor perspectives in biology* 3 (2011): a004168.

21. R. B. Stockbridge and R. Wolfenden, "The Intrinsic Reactivity of ATP and the Catalytic Proficiencies of Kinases Acting on Glucose, N-Acetylgalactosamine, and Homoserine," *Journal of Biological Chemistry* 284 (2009): 22747–22757, https://doi.org/10.1074/jbc.M109.017806.

22. J. Deng and A. Walther, "ATP-Responsive and ATP-Fueled Self-Assembling Systems and Materials," *Advanced Materials* 32 (2020): 2002629, https://doi.org/10.1002/adma.202002629.

23. N. Singh, G. J. M. Formon, S. De Piccoli, and T. M. Hermans, "Devising Synthetic Reaction Cycles for Dissipative Nonequilibrium Self-Assembly," *Advanced Materials* 32 (2020): 1906834, https://doi.org/10.1002/adma.201906834.

24. J. Leira-Iglesias, A. Sorrenti, A. Sato, P. A. Dunne, and T. M. Hermans, "Supramolecular Pathway Selection of Perylenediimides Mediated by Chemical Fuels," *Chemical Communications* 52 (2016): 9009–9012, https://doi.org/10.1039/C6CC01192F.

25. K. Jalani, S. Dhiman, A. Jain, and S. J. George, "Temporal Switching of an Amphiphilic Self-Assembly by a Chemical Fuel-Driven Conformational Response," *Chemical Science* 8 (2017): 6030–6036, https://doi.org/10.1039/C7SC01730H.

26. I. Maity, N. Wagner, R. Mukherjee, et al., "A Chemically Fueled Non-Enzymatic Bistable Network," *Nature Communications* 10 (2019): 4636, https://doi.org/10.1038/s41467-019-12645-0.

27. Y. Altay, I. A. B. Pijpers, L. K. E. A. Abdelmohsen, and J. C. M. van Hest, "Dynamic Assembly of Micellar Mesostructures," *ChemSystemsChem* 2 (2019): 1900049.

28. B. Fan, Y. Men, S. A. P. van Rossum, G. Li, and R. Eelkema, "A Fuel-Driven Chemical Reaction Network Based on Conjugate Addition and Elimination Chemistry," *ChemSystemsChem* 2 (2019): 1900028.

29. W. A. Ogden and Z. Guan, "Redox Chemical-Fueled Dissipative Self-Assembly of Active Materials," *ChemSystemsChem* 2 (2019): 1900030.

30. S. Yang, G. Schaeffer, E. Mattia, et al., "Chemical Fueling Enables Molecular Complexification of Self-Replicators**," *Angewandte Chemie International Edition* 60 (2021): 11344–11349, https://doi.org/10.1002/anie.202016196.

31. I. Colomer, S. M. Morrow, and S. P. Fletcher, "A Transient Self-Assembling Self-Replicator," *Nature Communications* 9 (2018): 2239, https://doi.org/10.1038/s41467-018-04670-2.

32. I. Colomer, A. Borissov, and S. P. Fletcher, "Selection from a Pool of Self-Assembling Lipid Replicators," *Nature Communications* 11 (2020): 176, https://doi.org/10.1038/s41467-019-13903-x.

33. C. Pezzato and L. J. Prins, "Transient Signal Generation in a Self-Assembled Nanosystem Fueled by ATP," *Nature Communications* 6 (2015): 7790, https://doi.org/10.1038/ncomms8790.

34. A. Sorrenti, J. Leira-Iglesias, A. Sato, and T. M. Hermans, "Non-Equilibrium Steady States in Supramolecular Polymerization," *Nature Communications* 8 (2017): 15899, https://doi.org/10.1038/ncomms15899.

16163028, 2026, 68, Downloaded from https://advanced.onlinelibrary.wiley.com/doi/10.1002/adfm.77237, Wiley Online Library on [17/11/2026]. See the Terms and Conditions (https://onlinelibrary.wiley.com/terms-and-conditions) on Wiley Online Library for rules of use; OA articles are governed by the applicable Creative Commons License

35. S. Dhiman, A. Jain, and S. J. George, "Transient Helicity: Fuel-Driven Temporal Control over Conformational Switching in a Supramolecular Polymer," *Angewandte Chemie International Edition* 56 (2017): 1329–1333, https://doi.org/10.1002/anie.201610946.

36. P. Solis Munana, G. Ragazzon, J. Dupont, C. Z. Ren, L. J. Prins, and J. L. Chen, "Substrate-Induced Self-Assembly of Cooperative Catalysts," *Angewandte Chemie International Edition* 57 (2018): 16469–16474, https://doi.org/10.1002/anie.201810891.

37. M. A. Cardona and L. J. Prins, "ATP-Fuelled Self-Assembly to Regulate Chemical Reactivity in the Time Domain," *Chemical Science* 11 (2019): 1518–1522, https://doi.org/10.1039/C9SC05188K.

38. L. Heinen and A. Walther, "Programmable Dynamic Steady States in ATP-Driven Nonequilibrium DNA Systems," *Science Advances* 5 (2019): aaw0590.

39. A. Englert, F. Majer, J. L. Schiessl, A. J. C. Kuehne, and M. von Delius, "Acylphosphates as Versatile Transient Species in Reaction Networks and Optical Catalyst Screenings," *Chem* 10 (2023): 910–923.

40. S. Maiti, I. Fortunati, C. Ferrante, P. Scrimin, and L. J. Prins, "Dissipative Self-Assembly of Vesicular Nanoreactors," *Nature Chemistry* 8 (2016): 725–731, https://doi.org/10.1038/nchem.2511.

41. M. Pol, K. Dai, R. Thomann, S. Moser, S. K. Roy, and C. G. Pappas, *Angewandte Chemie* 63 (2024): 202404360.

42. O. Zozulia, C. M. E. Kriebisch, B. A. K. Kriebisch, et al., "Acyl Phosphates as Chemically Fueled Building Blocks for Self-Sustaining Protocells," *Angewandte Chemie* 63 (2024): 202406094.

43. S. M. Poprawa, M. Stasi, B. A. K. Kriebisch, M. Wenisch, J. Sastre, and J. Boekhoven, "Active Droplets through Enzyme-free, Dynamic Phosphorylation," *Nature Communications* 15 (2024): 4204, https://doi.org/10.1038/s41467-024-48571-z.

44. C. G. Pappas, I. R. Sasselli, and R. V. Ulijn, "Biocatalytic Pathway Selection in Transient Tripeptide Nanostructures," *Angewandte Chemie International Edition* 54 (2015): 8119–8123, https://doi.org/10.1002/anie.201500867.

45. S. M. Poprawa, N. L. Hoja, C. Hipp, et al., "Enzyme-Free Phosphorylation with Kinetic Gating in a De Novo Coiled-Coil System," *Journal of the American Chemical Society* 148 (2026): 21725–21736, https://doi.org/10.1021/jacs.6c02162.

46. J. Boekhoven, W. E. Hendriksen, G. J. Koper, R. Eelkema, and J. H. van Esch, "Transient Assembly of Active Materials Fueled by a Chemical Reaction," *Science* 349 (2015): 1075–1079, https://doi.org/10.1126/science.aac6103.

47. B. G. P. van Ravensteijn, W. E. Hendriksen, R. Eelkema, J. H. van Esch, and W. K. Kegel, "Fuel-Mediated Transient Clustering of Colloidal Building Blocks," *Journal of the American Chemical Society* 139 (2017): 9763–9766.

48. L. S. Kariyawasam and C. S. Hartley, "Dissipative Assembly of Aqueous Carboxylic Acid Anhydrides Fueled by Carbodiimides," *Journal of the American Chemical Society* 139 (2017): 11949–11955, https://doi.org/10.1021/jacs.7b06099.

49. M. Wenisch, M. Stasi, S. M. Poprawa, B. A. K. Kriebisch, and J. Boekhoven, "Chemically Fueled, Active Droplets Prevent the Aging of Peptides into Amyloid-Like Fibers," *Journal of the American Chemical Society* 147 (2025): 42472–42481.

50. H. Soria-Carrera, L. Kauling, and J. Boekhoven, "Primitive Genotype-Phenotype Coupling in Fuel-Dependent Synthetic Cells with an Autocatalyst," *Chemistry* 12 (2025): 102816.

51. C. M. E. Kriebisch, B. A. K. Kriebisch, G. Hafner, et al., "Chemically Fueled Active Transport," *Angewandte Chemie International Edition* 64 (2025): 202500243, https://doi.org/10.1002/anie.202500243.

52. K. Liang, F. Nicoli, S. A. Shehimy, et al., "Catalysis-Driven Active Transport across a Liquid Membrane," *Angewandte Chemie International Edition* 64 (2025): 202421234, https://doi.org/10.1002/anie.202421234.

53. B. A. Kriebisch, C. M. Kriebisch, H. W. Swanson, et al., *Chem* 11 (2024): 102293, https://doi.org/10.1016/j.chempr.2024.08.016.

54. Y. Zhao, B. Wu, S. Sun, and P. Wu, "Chemical Fuel-Driven Stiffening of Transient Hydrogels via Vitrifiable Phase Separation," *Angewandte Chemie International Edition* 64 (2025): 202518064..

55. C. M. Kriebisch, B. A. Kriebisch, J. Langlais, et al., "The Multifunctional Role of Templates in Chemically Fueled Dynamic Combinatorial Libraries," *ChemSystemsChem* 7 (2025): 202400087.

56. I. Tsironi, J. A. Maleszka, B. A. Kriebisch, et al., "Fuel-Driven π-Conjugated Superstructures to Form Transient Conductive Hydrogels," *Angewandte Chemie* 137 (2025): 202417109, https://doi.org/10.1002/ange.202417109.

57. N. Ozbek, X. Chen, B. A. K. Kriebisch, et al., "Molecular Design in L -Glutamic Acid-Based Peptide Assembly Dynamics Driven by Carbodiimide-Fueled Reaction Cycle," *Biomacromolecules* 27 (2026): 1690–1697, https://doi.org/10.1021/acs.biomac.5c02255.

58. A. L. Holtmannspotter, X. Chen, Y. Fu, et al., "Design of Fuel-Dependent, Complex-Coacervate-Based Synthetic Cells," *Chemistry—A European Journal* (2026): 71099, https://doi.org/10.1002/chem.71099.

59. S. Bal, K. Das, S. Ahmed, and D. Das, "Chemically Fueled Dissipative Self-Assembly That Exploits Cooperative Catalysis," *Angewandte Chemie International Edition* 58 (2019): 244–247, https://doi.org/10.1002/anie.201811749.

60. R. K. Grotsch, C. Wanzke, M. Speckbacher, A. Angi, B. Rieger, and J. Boekhoven, "Pathway Dependence in the Fuel-Driven Dissipative Self-Assembly of Nanoparticles," *Journal of the American Chemical Society* 141 (2019): 9872–9878, https://doi.org/10.1021/jacs.9b02004.

61. S. Debnath, S. Roy, and R. V. Ulijn, "Peptide Nanofibers with Dynamic Instability through Nonequilibrium Biocatalytic Assembly," *Journal of the American Chemical Society* 135 (2013): 16789–16792, https://doi.org/10.1021/ja4086353.

62. L. Saile, K. Dai, M. D. Pol, T. Pramod, R. Thomann, and C. G. Pappas, "Chirality Makes or Breaks Chemically Driven Self-Assembly," *Angewandte Chemie International Edition* 64 (2025): 202508481, https://doi.org/10.1002/anie.202508481.

63. A. Jain, S. Dhiman, A. Dhayani, P. K. Vemula, and S. J. George, "Chemical Fuel-Driven Living and Transient Supramolecular Polymerization," *Nature Communications* 10 (2019): 450, https://doi.org/10.1038/s41467-019-08308-9.

64. C. S. Wood, C. Browne, D. M. Wood, and J. R. Nitschke, "Fuel-Controlled Reassembly of Metal–Organic Architectures," *ACS Central Science* 1 (2015): 504–509, https://doi.org/10.1021/acscentsci.5b00279.

65. N. Singh, B. Lainer, G. J. M. Formon, S. De Piccoli, and T. M. Hermans, "Re-Programming Hydrogel Properties Using a Fuel-Driven Reaction Cycle," *Journal of the American Chemical Society* 142 (2020): 4083–4087, https://doi.org/10.1021/jacs.9b11503.

66. M. P. van der Helm, C. L. Wang, B. Fan, M. Macchione, E. Mendes, and R. Eelkema, "Organocatalytic Control over a Fuel-Driven Transient-Esterification Network," *Angewandte Chemie* 59 (2020): 20604–20611.

67. H. Wang, S. Bai, G. Gu, C. Zhang, and Y. Wang, "Chemical Reaction Steers Spatiotemporal Self-Assembly of Supramolecular Hydrogels," *ChemPlusChem* 89 (2024): 202400396, https://doi.org/10.1002/cplu.202400396.

68. Z. Wang, X. Lin, X. Huang, et al., "A Highly Spatiotemporal Resolved Pyrometry for Combustion Temperature Measurement of Single Microparticles Applied in Powder-Fueled Ramjets," *Nanomaterials (Basel)* 15 (2025): 223.

69. Y. Xu, Y. Luo, X. Lu, et al., "Dynamic Modulation of Multicellular Interactions via ATP-Dissipative DNA Assembly," *Journal of the American Chemical Society* 147 (2025): 28277–28288, https://doi.org/10.1021/jacs.5c08925.

16163028, 2026, 68, Downloaded from https://advanced.onlinelibrary.wiley.com/doi/10.1002/adfm.77237, Wiley Online Library on [17/11/2026]. See the Terms and Conditions (https://onlinelibrary.wiley.com/terms-and-conditions) on Wiley Online Library for rules of use; OA articles are governed by the applicable Creative Commons License

70. S. Borsley, E. Kreidt, D. A. Leigh, and B. M. W. Roberts, "Autonomous Fuelled Directional Rotation about a Covalent Single Bond," *Nature* (2022): 80–85, https://doi.org/10.1038/s41586-022-04450-5.

71. S. Borsley, D. A. Leigh, and B. M. W. Roberts, "A Doubly Kinetically-Gated Information Ratchet Autonomously Driven by Carbodiimide Hydration," *Journal of the American Chemical Society* 143 (2021): 4414–4420, https://doi.org/10.1021/jacs.1c01172.

72. S. Amano, S. D. P. Fielden, and D. A. Leigh, "A Catalysis-driven Artificial Molecular Pump," *Nature* 594 (2021): 529–534, https://doi.org/10.1038/s41586-021-03575-3.

73. P. S. Schwarz, M. Tena-Solsona, K. Dai, and J. Boekhoven, "Carbodiimide-fueled Catalytic Reaction Cycles to Regulate Supramolecular Processes," *Chemical Communications* 58 (2022): 1284–1297, https://doi.org/10.1039/D1CC06428B.

74. X. Chen and M. A. Wurbser, "Chemically Fueled Supramolecular Materials," *Accounts of Materials Research* 4 (2023): 416–426, https://doi.org/10.1021/accountsmr.2c00244.

75. L. Wang, J. Yuan, and J. Hao, "Transient Self-assembly Driven by Chemical Fuels," *ChemPhysMater* 3 (2024): 1–23, https://doi.org/10.1016/j.chphma.2023.06.002.

76. M. Stasi, A. Monferrer, L. Babl, et al., "Regulating DNA-Hybridization Using a Chemically Fueled Reaction Cycle," *Journal of the American Chemical Society* 144 (2022): 21939–21947, https://doi.org/10.1021/jacs.2c08463.

77. E. Del Grosso, A. Amodio, G. Ragazzon, L. J. Prins, and F. Ricci, "Dissipative Synthetic DNA-Based Receptors for the Transient Loading and Release of Molecular Cargo," *Angewandte Chemie* 57 (2018): 10489–10493.

78. A. K. Dambenieks, P. H. Q. Vu, and T. M. Fyles, "Dissipative Assembly of a Membrane Transport System," *Chemical Science* 5 (2014): 3396–3403, https://doi.org/10.1039/C4SC01258E.

79. J. Heckel, S. Loescher, R. T. Mathers, and A. Walther, "Chemically Fueled Volume Phase Transition of Polyacid Microgels," *Angewandte Chemie International Edition* 60 (2021): 7117–7125, https://doi.org/10.1002/anie.202014417.

80. H. Xu, S. Bai, G. Gu, et al., "Bioinspired Self-Resettable Hydrogel Actuators Powered by a Chemical Fuel," *ACS Applied Materials & Interfaces* 14 (2022): 43825–43832, https://doi.org/10.1021/acsami.2c13368.

81. B. Zhang, I. M. Jayalath, J. Ke, J. L. Sparks, C. S. Hartley, and D. Konkolewicz, "Chemically Fueled Covalent Crosslinking of Polymer Materials," *Chemical Communications* 55 (2019): 2086–2089, https://doi.org/10.1039/C8CC09823A.

82. O. J. Dodo, L. Petit, C. W. H. Rajawasam, C. S. Hartley, and D. Konkolewicz, "Tailoring Lifetimes and Properties of Carbodiimide-Fueled Covalently Cross-linked Polymer Networks," *Macromolecules* 54 (2021): 9860–9867, https://doi.org/10.1021/acs.macromol.1c01586.

83. S. Amano, S. Borsley, D. A. Leigh, and Z. Sun, "Chemical Engines: Driving Systems away from Equilibrium through Catalyst Reaction Cycles," *Nature Nanotechnology* 16 (2021): 1057–1067, https://doi.org/10.1038/s41565-021-00975-4.

84. S. Amano, M. Esposito, E. Kreidt, D. A. Leigh, E. Penocchio, and B. M. W. Roberts, "Using Catalysis to Drive Chemistry Away from Equilibrium: Relating Kinetic Asymmetry, Power Strokes, and the Curtin–Hammett Principle in Brownian Ratchets," *Journal of the American Chemical Society* 144 (2022): 20153–20164, https://doi.org/10.1021/jacs.2c08723.

85. S. Kassem, T. van Leeuwen, A. S. Lubbe, M. R. Wilson, B. L. Feringa, and D. A. Leigh, "Artificial Molecular Motors," *Chemical Society Reviews* 46 (2017): 2592–2621, https://doi.org/10.1039/C7CS00245A.

86. R. D. Astumian, "How Molecular Motors Work—Insights from the Molecular Machinist's Toolbox: the Nobel Prize in Chemistry 2016," *Chemical Science* 8 (2017): 840–845, https://doi.org/10.1039/C6SC04806D.

87. R. D. Astumian, "Kinetic Asymmetry and Directionality of Nonequilibrium Molecular Systems," *Angewandte Chemie International Edition* 63 (2024): 202306569, https://doi.org/10.1002/anie.202306569.

88. G. Ragazzon and L. J. Prins, "Energy Consumption in Chemical Fuel-driven Self-assembly," *Nature Nanotechnology* 13 (2018): 882–889, https://doi.org/10.1038/s41565-018-0250-8.

89. T. Sangchai, S. Al Shehimy, E. Penocchio, and G. Ragazzon, "Artificial Molecular Ratchets: Tools Enabling Endergonic Processes," *Angewandte Chemie International Edition* 62 (2023): 202309501, https://doi.org/10.1002/anie.202309501.

90. S. Erbas-Cakmak, D. A. Leigh, C. T. McTernan, and A. L. Nussbaumer, "Artificial Molecular Machines," *Chemical Reviews* 115 (2015): 10081–10206, https://doi.org/10.1021/acs.chemrev.5b00146.

91. R. D. Astumian, "Irrelevance of the Power Stroke for the Directionality, Stopping Force, and Optimal Efficiency of Chemically Driven Molecular Machines," *Biophysical Journal* 108 (2015): 291–303, https://doi.org/10.1016/j.bpj.2014.11.3459.

92. R. D. Astumian, S. Mukherjee, and A. Warshel, "The Physics and Physical Chemistry of Molecular Machines," *Chemphyschem* 17 (2016): 1719–1741, https://doi.org/10.1002/cphc.201600184.

93. S. Borsley, D. Leigh, and B. M. W. Roberts, "Molecular Ratchets and Kinetic Asymmetry: Giving Chemistry Direction," *Angewandte Chemie* 63 (2024): 202400495.

94. A. J. Bissette and S. P. Fletcher, "Novel Applications of Physical Autocatalysis," *Origins of Life and Evolution of Biospheres* 45 (2015): 21–30, https://doi.org/10.1007/s11084-015-9404-y.

95. S. M. Morrow, I. Colomer, and S. P. Fletcher, "A Chemically Fuelled Self-Replicator," *Nature Communications* 10 (2019): 1011, https://doi.org/10.1038/s41467-019-08885-9.

96. M. Tena-Solsona, B. Riess, R. K. Grotsch, et al., "Non-equilibrium Dissipative Supramolecular Materials with a Tunable Lifetime," *Nature Communications* 8 (2017): 15895, https://doi.org/10.1038/ncomms15895.

97. M. Tena-Solsona, C. Wanzke, B. Riess, A. R. Bausch, and J. Boekhoven, "Self-Selection of Dissipative Assemblies Driven by Primitive Chemical Reaction Networks," *Nature Communications* 9 (2018): 2044, https://doi.org/10.1038/s41467-018-04488-y.

98. B. Riess, C. Wanzke, M. Tena-Solsona, R. K. Grotsch, C. Maity, and J. Boekhoven, "Dissipative Assemblies That Inhibit Their Deactivation," *Soft Matter* 14 (2018): 4852–4859, https://doi.org/10.1039/C8SM00822A.

99. T. E. Creighton, "Protein Folding," *Biochemical Journal* 270 (1990): 1–16, https://doi.org/10.1042/bj2700001.

100. L. Szilak, J. Moitra, and C. Vinson, "Design of a Leucine Zipper Coiled Coil Stabilized 1.4 Kcal Mol $^{-1}$ by Phosphorylation of a Serine in the E Position," *Protein Science* 6 (1997): 1273–1283, https://doi.org/10.1002/pro.5560060615.

101. A. Bah, R. M. Vernon, Z. Siddiqui, et al., "Folding of an Intrinsically Disordered Protein by Phosphorylation as a Regulatory Switch," *Nature* 519 (2015): 106–109, https://doi.org/10.1038/nature13999.

102. E. Spatola, F. Rispoli, D. Del Giudice, et al., "Dissipative Control of the Fluorescence of a 1,3-dipyrenyl Calix[4]Arene in the Cone Conformation," *Organic & Biomolecular Chemistry* 20 (2021): 132–138, https://doi.org/10.1039/D1OB02096J.

103. Z. Zong, Q. Zhang, S. H. Qiu, et al., "Dynamic Timing Control over Multicolor Molecular Emission by Temporal Chemical Locking," *Angewandte Chemie International Edition* 61 (2022): 202116414, https://doi.org/10.1002/anie.202116414.

104. M. Schliwa and G. Woehlke, "Molecular Motors," *Nature* 422 (2003): 759–765, https://doi.org/10.1038/nature01601.

105. C. Pezzato, C. Cheng, J. F. Stoddart, and R. D. Astumian, "Mastering the Non-Equilibrium Assembly and Operation of Molecular Machines," *Chemical Society Reviews* 46 (2017): 5491–5507, https://doi.org/10.1039/C7CS00068E.

106. S. A. Vignon, T. Jarrosson, T. Iijima, H. R. Tseng, J. K. Sanders, and J. F. Stoddart, "Switchable Neutral Bistable Rotaxanes," *Journal of the*

16163028, 2026, 68, Downloaded from https://advanced.onlinelibrary.wiley.com/doi/10.1002/adfm.77237, Wiley Online Library on [17/11/2026]. See the Terms and Conditions (https://onlinelibrary.wiley.com/terms-and-conditions) on Wiley Online Library for rules of use; OA articles are governed by the applicable Creative Commons License

American Chemical Society 126 (2004): 9884–9885, https://doi.org/10.1021/ja048080k.

107. D. S. Marlin, D. G. Cabrera, D. A. Leigh, and A. M. Slawin, "An Allosterically Regulated Molecular Shuttle," *Angewandte Chemie International Edition* 45 (2006): 1385–1390, https://doi.org/10.1002/anie.200502624.

108. C. Cheng, P. R. McGonigal, S. T. Schneebeli, et al., "An Artificial Molecular Pump," *Nature Nanotechnology* 10 (2015): 547–553, https://doi.org/10.1038/nnano.2015.96.

109. J. D. Badjic, V. Balzani, A. Credi, S. Silvi, and J. F. Stoddart, "A Molecular Elevator," *Science* 303 (2004): 1845–1849, https://doi.org/10.1126/science.1094791.

110. J. D. Badjic, C. M. Ronconi, J. F. Stoddart, V. Balzani, S. Silvi, and A. Credi, "Operating Molecular Elevators," *Journal of the American Chemical Society* 128 (2006): 1489–1499, https://doi.org/10.1021/ja0543954.

111. J. Wu, K. C. Leung, D. Benitez, et al., "An Acid–Base-Controllable [c2]Daisy Chain," *Angewandte Chemie International Edition* 47 (2008): 7470–7474, https://doi.org/10.1002/anie.200803036.

112. P. L. Wang, S. Borsley, M. J. Power, A. Cavasso, N. Giuseppone, and D. A. Leigh, "Transducing Chemical Energy through Catalysis by an Artificial Molecular Motor," *Nature* 637 (2025): 594–600, https://doi.org/10.1038/s41586-024-08288-x.

113. P. Z. Wang, W. J. Xiao, and J. R. Chen, "Light-empowered Contra-Thermodynamic Stereochemical Editing," *Nature Reviews Chemistry* 7 (2023): 35–50, https://doi.org/10.1038/s41570-022-00441-2.

114. S. Borsley, J. M. Gallagher, D. A. Leigh, and B. M. W. Roberts, "Ratcheting Synthesis," *Nature Reviews Chemistry* 8 (2024): 8–29, https://doi.org/10.1038/s41570-023-00558-y.

115. A. S. Spirin and A. V. Finkelstein, *Molecular Machines in Biology: Workshop of the Cell*, ed. J. Frank, (Cambridge Univ. Press, 2012).

116. H. Khatter, A. G. Myasnikov, S. K. Natchiar, and B. P. Klaholz, "Structure of the human 80S Ribosome," *Nature* 520 (2015): 640–645, https://doi.org/10.1038/nature14427.

117. E. Olivieri, J. M. Gallagher, A. Betts, T. W. Mrad, and D. A. Leigh, "Endergonic Synthesis Driven by Chemical Fuelling," *Nature Synthesis* 3 (2024): 707–714.

118. S. Al Shehimy, H.-D. Le, S. Di Noja, S. Amano, L. Monari, and G. Ragazzon, "Endergonic Synthesis of Diels-Alder Adducts Enables Non-equilibrium Adaptive Behaviors in Chemical Reaction Networks," *Angewandte Chemie* 63 (2024): e202411554, https://doi.org/10.1002/anie.202411554.

119. B. Rieß, R. K. Grötsch, and J. Boekhoven, "The Design of Dissipative Molecular Assemblies Driven by Chemical Reaction Cycles," *Chemistry* 6 (2020): 552–578.

120. B. Rieß and J. Boekhoven, "Applications of Dissipative Supramolecular Materials with a Tunable Lifetime," *ChemNanoMat* 4 (2018): 710–719.

121. B. A. Kriebisch, C. M. Kriebisch, A. M. Bergmann, C. Wanzke, M. Tena-Solsona, and J. Boekhoven, "Tuning the Kinetic Trapping in Chemically Fueled Self-Assembly," *ChemSystemsChem* 5 (2023): 202200035.

122. J. Leira-Iglesias, A. Tassoni, T. Adachi, M. Stich, and T. M. Hermans, "Oscillations, Travelling Fronts and Patterns in a Supramolecular System," *Nature Nanotechnology* 13 (2018): 1021–1027, https://doi.org/10.1038/s41565-018-0270-4.

123. J. Rodon-Fores, M. A. Wurbser, M. Kretschmer, et al., "A Chemically Fueled Supramolecular Glue for Self-Healing Gels," *Chemical Science* 13 (2022): 11411–11421, https://doi.org/10.1039/D2SC03691F.

124. X. Chen, M. Stasi, J. Rodon-Fores, et al., "A Carbodiimide-Fueled Reaction Cycle That Forms Transient 5(4 H)-Oxazolones," *Journal of the American Chemical Society* 145 (2023): 6880–6887, https://doi.org/10.1021/jacs.3c00273.

125. J. Heckel, F. Batti, R. T. Mathers, and A. Walther, "Spinodal Decomposition of Chemically Fueled Polymer Solutions," *Soft Matter* 17 (2021): 5401–5409, https://doi.org/10.1039/D1SM00515D.

126. C. Donau, F. Spath, M. Sosson, et al., "Active Coacervate Droplets as a Model for Membraneless Organelles and Protocells," *Nature Communications* 11 (2020): 5167, https://doi.org/10.1038/s41467-020-18815-9.

127. M. Wenisch, M. Stasi, S. M. Poprawa, B. A. Kriebisch, and J. Boekhoven, "Chemically Fueled, Active Droplets Prevent the Aging of Peptides into Amyloid-Like Fibers," *Journal of the American Chemical Society* 147 (2025): 42472–42481.

128. M. Wenisch, Y. Li, M. G. Braun, et al., "Toward Synthetic Life—Emergence, Growth, Creation of Offspring, Decay, and Rescue of Fuel-dependent Synthetic Cells," *Chemistry* 11 (2025): 102578.

129. C. Sharma, A. Samanta, R. S. Schmidt, and A. Walther, "DNA-Based Signaling Networks for Transient Colloidal Co-Assemblies," *Journal of the American Chemical Society* 145 (2023): 17819–17830, https://doi.org/10.1021/jacs.3c04807.

130. C. Wanzke, M. Tena-Solsona, B. Rieß, L. Tebcharani, and J. Boekhoven, "Active Droplets in a Hydrogel Release Drugs with a Constant and Tunable Rate," *Materials Horizons* 7 (2020): 1397–1403, https://doi.org/10.1039/C9MH01822K.

131. P. S. Schwarz, L. Tebcharani, J. E. Heger, P. Muller-Buschbaum, and J. Boekhoven, "Chemically Fueled Materials with a Self-immolative Mechanism: Transient Materials with a Fast On/off Response," *Chemical Science* 12 (2021): 9969–9976, https://doi.org/10.1039/D1SC02561A.

132. C. Wanzke, A. Jussupow, F. Kohler, H. Dietz, V. R. I. Kaila, and J. Boekhoven, "Dynamic Vesicles Formed by Dissipative Self-Assembly," *ChemSystemsChem* 2 (2019): 1900044.

133. A. Fracassi, A. Seoane, R. J. Brea, H.-G. Lee, A. Harjung, and N. K. Devaraj, "Abiotic Lipid Metabolism Enables Membrane Plasticity in Artificial Cells," *Nature Chemistry* 17 (2025): 799–807.

134. M. A. Würbser, P. S. Schwarz, J. Heckel, A. M. Bergmann, A. Walther, and J. Boekhoven, "Chemically Fueled Block Copolymer Self-Assembly into Transient Nanoreactors," *ChemSystemsChem* 3 (2021): 2100015.

135. F. Schnitter, B. Riess, C. Jandl, and J. Boekhoven, "Memory, Switches, and an OR-port through Bistability in Chemically Fueled Crystals," *Nature Communications* 13 (2022): 2816, https://doi.org/10.1038/s41467-022-30424-2.

136. K. Das, L. Gabrielli, and L. J. Prins, "Chemically Fueled Self-Assembly in Biology and Chemistry," *Angewandte Chemie International Edition* 60 (2021): 20120–20143, https://doi.org/10.1002/anie.202100274.

137. L. Blanchoin, T. Pollard, and R. Mullins, "Interactions of ADF/Cofilin, Arp2/3 Complex, Capping Protein and Profilin in Remodeling of Branched Actin Filament Networks," *Current Biology* 10 (2000): 1273–1282, https://doi.org/10.1016/S0960-9822(00)00749-1.

138. M. A. Wear, D. A. Schafer, and J. A. Cooper, "Actin Dynamics: Assembly and Disassembly of Actin Networks," *Current Biology* 10 (2000): R891–R895, https://doi.org/10.1016/S0960-9822(00)00845-9.

139. M. Cheng, D. Chen, L. Zhang, T. Xiao, J. Jiang, and L. Wang, "Chemical Fuel-Driven Gelation with Dissipative Assembly-Induced Emission," *Organic Chemistry Frontiers* 10 (2023): 1380–1385, https://doi.org/10.1039/D2QO01888H.

140. Q. Wang, Q. Zhang, Q. W. Zhang, et al., "Color-tunable Single-Fluorophore Supramolecular System with Assembly-Encoded Emission," *Nature Communications* 11 (2020): 158, https://doi.org/10.1038/s41467-019-13994-6.

141. M. A. Cardona, R. Chen, S. Maiti, et al., "Time-Gated Fluorescence Signalling under Dissipative Conditions," *Chemical Communications* 56 (2020): 13979–13982, https://doi.org/10.1039/D0CC05993E.

142. J. Deng and A. Walther, "Programmable ATP-Fueled DNA Coacervates by Transient Liquid-Liquid Phase Separation," *Chemistry* 6 (2020): 3329–3343, https://doi.org/10.1016/j.chempr.2020.09.022.

16163028, 2026, 68, Downloaded from https://advanced.onlinelibrary.wiley.com/doi/10.1002/adfm.77237, Wiley Online Library on [17/11/2026]. See the Terms and Conditions (https://onlinelibrary.wiley.com/terms-and-conditions) on Wiley Online Library for rules of use; OA articles are governed by the applicable Creative Commons License

143. A. Goldbeter, "Dissipative Structures in Biological Systems: Bistability, Oscillations, Spatial Patterns and Waves," *Philosophical Transactions, Series A, Mathematical, Physical, and Engineering Sciences* 376 (2018): 20170376.

144. A. M. Turing, "The Chemical Basis of Morphogenesis," *Philosophical Transactions of the Royal Society of London Series B, Biological Sciences* 237 (1952): 37–72, https://doi.org/10.1098/rstb.1952.0012.

145. M. G. Howlett, A. H. J. Engwerda, R. J. H. Scanes, and S. P. Fletcher, "An Autonomously Oscillating Supramolecular Self-replicator," *Nature Chemistry* 14 (2022): 805–810, https://doi.org/10.1038/s41557-022-00949-6.

146. W. Zeng, C. Fan, X. Xing, et al., "Out of Equilibrium Coil-Helix Transition Driven by Chemical Fuels," *Giant* 7 (2021): 100067.

147. R. K. Grotsch, A. Angi, Y. G. Mideksa, et al., "Dissipative Self-Assembly of Photoluminescent Silicon Nanocrystals," *Angewandte Chemie International Edition* 57 (2018): 14608–14612, https://doi.org/10.1002/anie.201807937.

148. B. Klemm, R. W. Lewis, I. Piergentili, and R. Eelkema, "Temporally Programmed Polymer—Solvent Interactions Using a Chemical Reaction Network," *Nature Communications* 13 (2022): 6242, https://doi.org/10.1038/s41467-022-33810-y.

149. X. Lang, U. Thumu, L. Yuan, et al., "Chemical Fuel-Driven Transient Polymeric Micelle Nanoreactors toward Reversible Trapping and Reaction Acceleration," *Chemical Communications* 57 (2021): 5786–5789, https://doi.org/10.1039/D1CC00726B.

150. R. W. Lewis, B. Klemm, M. Macchione, and R. Eelkema, "Fuel-Driven Macromolecular Coacervation in Complex Coacervate Core Micelles," *Chemical Science* 13 (2022): 4533–4544, https://doi.org/10.1039/D2SC00805J.

151. C. Pan, J. Xu, L. Wang, et al., "Biocompatible Chemically Fueled Transient Polymer Nanoparticles for Temporally Programmable in Vivo Imaging," *CCS Chemistry* 5: 669–681, https://doi.org/10.31635/ccschem.022.202201893.

152. J. Li, L. Wang, C. Pan, B. Yang, and Y. Li, "Transient Biomacromolecular Nanoparticles for Labels with Self-Erasable and Rewritable Ability," *ChemSystemsChem* 5 (2023): 202200036.

153. V. W. Liyana Gunawardana, T. J. Finnegan, C. E. Ward, C. E. Moore, and J. D. Badjic, "Dissipative Formation of Covalent Basket Cages," *Angewandte Chemie International Edition* 61 (2022): 202207418, https://doi.org/10.1002/anie.202207418.

154. C. W. H. Rajawasam, C. Tran, M. Weeks, et al., "Chemically Fueled Reinforcement of Polymer Hydrogels," *Journal of the American Chemical Society* 145 (2023): 5553–5560, https://doi.org/10.1021/jacs.3c00668.

155. S. E. Gleeson, Z. Fink, P. D. Ashby, T. P. Russell, and B. A. Helms, "Transient Structuring of Liquids Using Dissipative Interfacial Assemblies," *Matter* 7 (2024): 1092–1105, https://doi.org/10.1016/j.matt.2023.12.025.

156. S. Bai, X. Niu, H. Wang, et al., "Chemical Reaction Powered Transient Polymer Hydrogels for Controlled Formation and Free Release of Pharmaceutical Crystals," *Chemical Engineering Journal* 414 (2021): 128877.

157. X. Lang, M. Zou, K. Wang, and H. Zhao, "Transient Compartmentalization in Coacervates Driven by Chemically Fueled Autocatalysis and Interfacial Remodeling," *Journal of the American Chemical Society* 148 (2026): 5357–5367.

158. Y. Zhao, B. Wu, S. Sun, and P. Wu, "Chemical Fuel-Driven Stiffening of Transient Hydrogels via Vitrifiable Phase Separation," *Angewandte Chemie* 64 (2025): 202518064, https://doi.org/10.1002/anie.202518064.

159. M. Cheng, C. Qian, Y. Ding, et al., "Writable and Self-Erasable Hydrogel Based on Dissipative Assembly Process from Multiple Carboxyl Tetraphenylethylene Derivative," *ACS Materials Letters* 2 (2020): 425–429, https://doi.org/10.1021/acsmaterialslett.9b00509.

160. S. Nikfarjam, R. Gibbons, F. Burni, S. R. Raghavan, M. A. Anisimov, and T. J. Woehl, "Chemically Fueled Dissipative Cross-Linking of Protein Hydrogels Mediated by Protein Unfolding," *Biomacromolecules* 24 (2023): 1131–1140, https://doi.org/10.1021/acs.biomac.2c01186.

161. T. J. Roberts, C. M. Eng, D. A. Sleboda, et al., "The Multi-Scale, Three-Dimensional Nature of Skeletal Muscle Contraction," *Physiology* 34 (2019): 402–408, https://doi.org/10.1152/physiol.00023.2019.

Biographies



Brigitte A. K. Kriebisch graduated in Chemistry in 2019 from the Technical University of Munich. She obtained her master's degree under the guidance of Prof. Boekhoven in 2019 at the same university. After that, she continued her studies as a Ph.D. student in Prof. Boekhoven's lab and defended her Ph.D. thesis *summa cum laude*, focusing on understanding and tuning the reciprocal coupling between chemically fueled reaction cycles and self-assemblies.

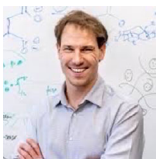

Prof. Dr. Job Boekhoven is developing tools to regulate molecular self-assembly inspired by biological processes. He is best known for introducing chemically fueled reaction cycles that control molecular assembly and phase separation, which open the door to exciting new properties, such as controllable lifetimes, catalysis, bistability, and self-healing. Moreover, the chemically fueled assemblies exhibit features we usually associate with living cells, such as emergence, decay, and self-division. He obtained a Ph.D. degree (2012) from Delft University of Technology and is currently an associate professor at the Technical University of Munich.

16163028, 2026, 68, Downloaded from https://advanced.onlinelibrary.wiley.com/doi/10.1002/adfm.77237, Wiley Online Library on [17/11/2026]. See the Terms and Conditions (https://onlinelibrary.wiley.com/terms-and-conditions) on Wiley Online Library for rules of use; OA articles are governed by the applicable Creative Commons License